

Review

# State-of-the-Art Review of Oxidative Dehydrogenation of Ethane to Ethylene over MoVNbTeO<sub>x</sub> Catalysts

Yuxin Chen , Binhang Yan  and Yi Cheng \*

Department of Chemical Engineering, Tsinghua University, Beijing 100084, China

\* Correspondence: yicheng@tsinghua.edu.cn

**Abstract:** Ethylene is mainly produced by steam cracking of naphtha or light alkanes in the current petrochemical industry. However, the high-temperature operation results in high energy demands, high cost of gas separation, and huge CO<sub>2</sub> emissions. With the growth of the verified shale gas reserves, oxidative dehydrogenation of ethane (ODHE) becomes a promising process to convert ethane from underutilized shale gas reserves to ethylene at a moderate reaction temperature. Among the catalysts for ODHE, MoVNbTeO<sub>x</sub> mixed oxide has exhibited superior catalytic performance in terms of ethane conversion, ethylene selectivity, and/or yield. Accordingly, the process design is compact, and the economic evaluation is more favorable in comparison to the mature steam cracking processes. This paper aims to provide a state-of-the-art review on the application of MoVNbTeO<sub>x</sub> catalysts in the ODHE process, involving the origin of MoVNbTeO<sub>x</sub>, (post-) treatment of the catalyst, material characterization, reaction mechanism, and evaluation as well as the reactor design, providing a comprehensive overview of M1 MoVNbTeO<sub>x</sub> catalysts for the oxidative dehydrogenation of ethane, thus contributing to the understanding and development of the ODHE process based on MoVNbTeO<sub>x</sub> catalysts.

**Keywords:** oxidative dehydrogenation of ethane; MoVNbTeO<sub>x</sub>; catalyst; ethylene; redox process



**Citation:** Chen, Y.; Yan, B.; Cheng, Y. State-of-the-Art Review of Oxidative Dehydrogenation of Ethane to Ethylene over MoVNbTeO<sub>x</sub> Catalysts. *Catalysts* **2023**, *13*, 204. <https://doi.org/10.3390/catal13010204>

Academic Editors: Hugo de Lasa and Mohammad Mozahar Hossain

Received: 19 December 2022

Revised: 6 January 2023

Accepted: 11 January 2023

Published: 16 January 2023



**Copyright:** © 2023 by the authors. Licensee MDPI, Basel, Switzerland. This article is an open access article distributed under the terms and conditions of the Creative Commons Attribution (CC BY) license (<https://creativecommons.org/licenses/by/4.0/>).

## 1. Introduction

Ethylene is one of the main building blocks for the production of value-added chemicals such as styrene, ethylene oxide, and polyethylene in the chemical industry. Currently, ethylene is mainly produced by steam cracking of naphtha or light alkanes, which is usually operated at high temperatures (800–900 °C), resulting in higher energy consumption and huge CO<sub>2</sub> emissions. With the growing concern about global warming, more efforts still need to be devoted to the development of new processes that can reduce CO<sub>2</sub> emissions during ethylene production.

In the last decade, the verified huge shale gas reserves have given the ethylene industry a new opportunity. Due to the shale revolution, the feedstock for ethylene production in North America has shifted from heavy petroleum to light ethane [1]. As a matter of fact, ethane is the second most abundant component in shale gas and natural gas. There are several ways to convert ethane to ethylene: (1) non-oxidative dehydrogenation of ethane to ethylene, (2) direct dehydrogenation of ethane to ethylene with hydrogen combustion, and (3) oxidative dehydrogenation of ethane (ODHE). Compared with the non-oxidative dehydrogenation of ethane and steam cracking method, ODHE is an exothermic reaction, which is thermodynamically favorable and operated under mild conditions (300–500 °C). Due to the introduced oxygen atmosphere, there is no coke formation during the ODHE process, allowing for long-term stable operation.

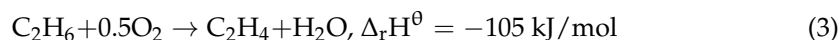
Non-oxidative dehydrogenation of ethane:



Hydrogen combustion:



## Oxidative dehydrogenation of ethane:



As shown in Figure 1, Gaffney et al. [1] conducted the process simulations for both the conventional steam cracking process and the novel ODHE process. The results show that OHDE is economically favorable. The process can minimize by-products and energy requirements, with less requirement for separation units, which can significantly reduce CO<sub>2</sub> emissions. Transition metal oxides have been widely used in the study of several catalytic systems due to their unique reaction properties [2–5]. In the past decades, several catalysts have been applied for the catalytic conversion of ethane by the ODHE process. And among all of them, the MoV(Sb/Te)(Nb) mixed oxides seem to be the most promising one, which can reach a high ethylene yield at mild conditions. Nevertheless, commercial implementation of the ODHE process is not yet available due to the superior economics of the steam cracking process of ethane. It is acknowledged that efforts are needed to meet several key requirements simultaneously [6–9]: long-term stability, ethylene yield > 70%, and ethylene productivity > 1.0 kg<sub>C<sub>2</sub>H<sub>4</sub></sub>/kg<sub>cat</sub>/h under 500 °C. One of the factors that limits the practical application of ODHE is the performance of the catalyst. Typically, the mixed oxide with the composition Mo-V-Te-Nb has the most excellent catalytic activity in the ODHE process, which is composed of M1, M2, and some minor phases [10,11]. It is widely accepted that the M1 phase is the most active phase for the conversion of alkanes, which follows the MvK redox mechanism, and the V<sup>5+</sup> in the (001) plane is the active site [12]. However, due to the complexity of the M1 MoVTeNbO<sub>x</sub> catalyst, there is limited or even conflicting understanding of the catalyst [13–18], which limits the rational understanding and development of the MoVTeNbO<sub>x</sub> catalyst.

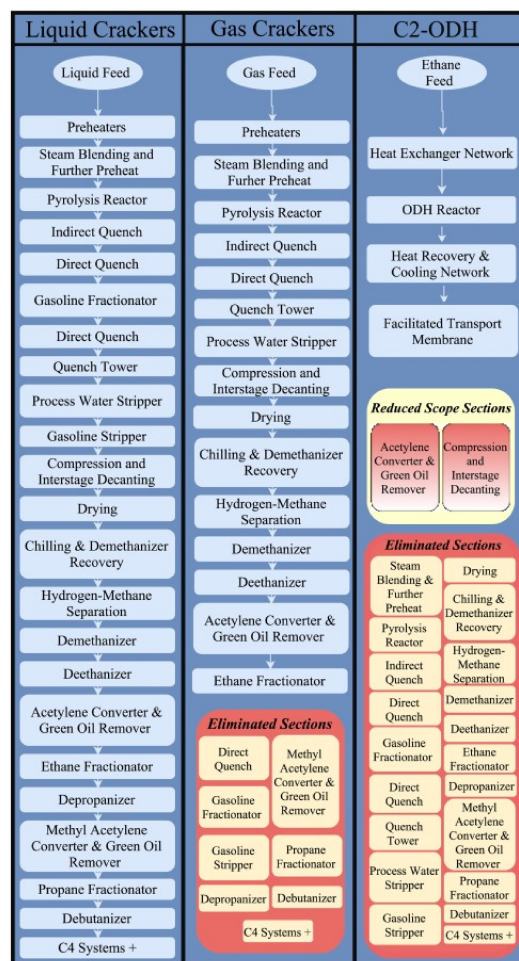


**Figure 1.** Scheme of conventional steam cracking vs. ODH unit operations. Adapted from ref. [1], Copyright (2017), with permission from Elsevier.

In the past decade, our group has devoted a lot of work in the field of the ODHE process based on M1 MoVNbTeO<sub>x</sub> catalysts [17–31], including catalyst mechanism unveiling, performance enhancement, reactor development, etc. Based on our research work and understanding in this field, this review mainly focuses on the research and development activities on the catalyst of M1 MoVNbTeO<sub>x</sub> applied in the ODHE process in the past 10 years, as well as the related work applied to the selective oxidation of other light alkanes based on MoV-M1 type catalysts. This review expects to provide a more comprehensive summary and analysis of the application of M1 MoVNbTeO<sub>x</sub> catalysts in the selective oxidation of light alkanes, especially in the oxidative dehydrogenation of ethane, so as to provide a more rational understanding of M1 MoVNbTeO<sub>x</sub> catalysts and promote the development of the ODHE process based on M1 MoVNbTeO<sub>x</sub> catalysts.

## 2. M1 MoVNbTeO<sub>x</sub> Catalyst for the ODHE Process

The first application of Mo-V-O(X) mixed oxide systems in the ODHE process can be dated back to 1978 [32]. After that, numerous researchers have conducted a lot of research on the application of this type of catalyst to the conversion of light alkanes (C<sub>2</sub>–C<sub>4</sub>). The Union Carbide Corporation published a patent about a Mo-V-Nb-Sb-X catalyst system for ODHE to ethylene in 1984 [33]. In the 1900s, the multi-component Mo-V-Nb-Te(Sb) catalysts were first discovered by Mitsubishi Chemical Corporation in the study of catalytic processes used for the selective oxidation of propane to acrylonitrile and acrylic acid [34–36], which also showed superior catalytic performance for oxidative dehydrogenation of ethane [37,38]. In the following two decades, the MoVNbTeO<sub>x</sub> has been widely used as an efficient catalyst for the selective oxidation of light alkanes, mainly for the selective oxidation of ethane to ethylene [37] and propane to acrylic acid [39] or acrylonitrile [40]. With the shale revolution, a growing number of researchers have focused their attention on the ODHE process based on mixed metal oxides of MoVNbTeO<sub>x</sub>.

Typically, MoVNbTeO<sub>x</sub> catalyst is prepared by hydrothermal [40] or slurry [41] method, which consists mainly of two phases, identified as orthorhombic M1 phase and pseudo-hexagonal M2 phase [42] (as shown in Figure 2), with other oxide phases in small amounts [42–47].

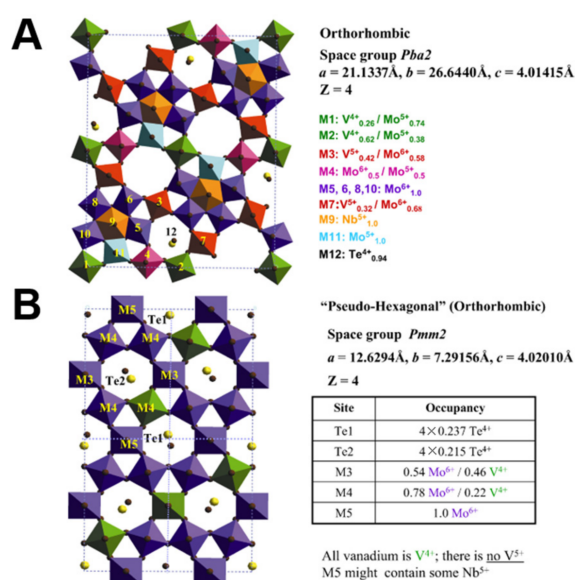


**Figure 2.** Scheme of (A) Structure of Mo<sub>7.8</sub>V<sub>1.2</sub>NbTe<sub>0.94</sub>O<sub>29</sub> (M1 phase), and (B) Structure of Mo<sub>4.67</sub>V<sub>1.33</sub>Te<sub>1.82</sub>O<sub>19.82</sub> (M2 phase). Adapted from ref. [42], Copyright (2004), with permission from Elsevier.

As shown in Figure 3, the M1 phase is a rod-like crystal preferentially growing along the *c*-axis and has been identified as an orthorhombic structure [43,44] with slabs consisting

of a network of  $\text{MO}_6$  octahedra stacked along the  $c$ -axis to form pentagonal, hexagonal, and heptagonal channels, which are the only active phase in the Mo-V-Nb-Te(Sb) catalyst for the ODHE process [48,49]. The M2 phase, with the lack of  $\text{V}^{5+}$  sites, is inactive for the C-H in alkanes but superior in the activation of propylene to acrylonitrile due to the enriched  $\text{Te}^{4+}$  sites. It is reported that the M2 phase shows synergy with the M1 phase in the oxidation of propane to acrylic acid [50] and propane ammoxidation to acrylonitrile [51–53]. To obtain a phase-pure M1  $\text{MoVNbTeO}_x$  catalyst, the M2 phase can be removed by being dissolved in either  $\text{H}_2\text{O}_2$  [54,55] or  $\text{HNO}_3$  [56] solutions.

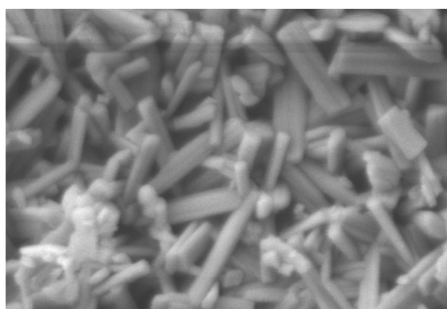


**Figure 3.** SEM image of rod-like morphology of M1  $\text{MoVNbTeO}_x$  catalyst.

Due to the complexity of the M1  $\text{MoVNbTeO}_x$  catalyst, its synthesis process needs to be precisely controlled, and the underlying reaction mechanism and active nature are still not well understood [57–59]. Relatively speaking, it is accepted that the M1 phase is the most active phase in the  $\text{MoVNbTeO}_x$ , and the  $\text{V}^{5+}$  sites in the basal (001) plane are the active sites responsible for the cleavage of the C-H bond in ethane. This catalytic process may follow the Mars-van Krevelen (MvK) redox mechanism with the involvement of lattice oxygen in the redox process, and the reduced oxygen vacancies are replenished by gas phase oxygen [55,57,60,61], as shown in Figure 4. The following sections will illustrate the synthesis method, structural properties, active nature, and reaction mechanism. Furthermore, Melzer et al. [16] demonstrated that the active site could also be exposed on the (120) and (210) facets, which may strongly depend on the morphology of the M1 phase [62].

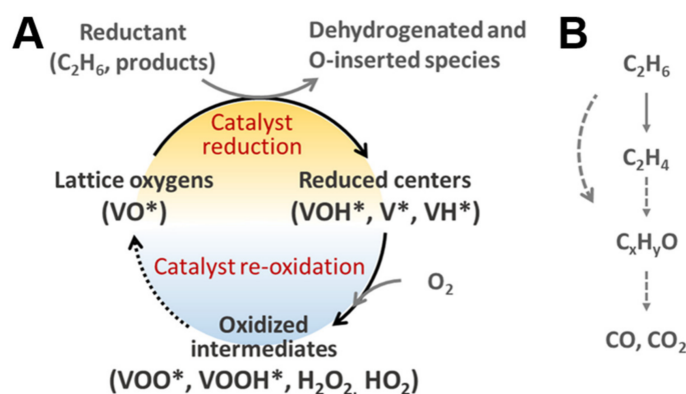


**Figure 4.** (A) Catalytic redox cycles, and (B)  $\text{C}_2\text{H}_6$  conversions involved in  $\text{C}_2\text{H}_6$ - $\text{O}_2$  reactions on vanadium oxide. Adapted from ref. [57], Copyright (2021), with permission from John Wiley & Sons.

### 2.1. The Role of Different Elements in the M1 Orthorhombic Structure

The square structure of M1 can be present in binary, ternary, or quaternary components composed of  $\text{MoV}(\text{Nb})(\text{Te}/\text{Sb})\text{O}_x$ . The group of Ueda [63] successfully synthesized five single-phase Mo-V-O based metal oxide catalysts with orthorhombic structure, Mo-V-O, Mo-V-Te-O, Mo-V-Sb-O, Mo-V-Te-Nb-O, and Mo-V-Sb-Nb-O catalysts. All of them were used as catalysts in the reaction of propane ammonia oxidation to acrylonitrile. They suggested that Mo and V in the octahedra network are responsible for the activation of

alkane, while Te or Sb plays an important role in the formation of alkenes. Nb is mainly acted as a diluter to separate the V sites in the network, which brings high selectivity of MoVNbTeO<sub>x</sub> catalysts. Moreover, the presence of Nb in the M1 phase stabilizes the catalyst structure from oxidation and reduction and allows very strong oxidation or reduction of the catalyst to be more easily recovered to its original value [64]. Deniau et al. [65] have investigated the influence of Te or Sb on the catalytic properties of the M1 phase of MoVTe(Sb)NbO<sub>x</sub> catalysts in ODHE. The results showed that the Te-containing catalyst has higher catalytic performance. The reason is that the Sb tends to stabilize vanadium in a reduced state, which results in a less active site (V<sup>5+</sup>). Girgsdies et al. [66] investigated the phase crystallization process of amorphous MoVTeNb oxide catalyst precursors during the calcination process by using in situ X-ray diffraction technique. The results indicated that the availability of Te plays a dominant role in the phase distribution of the final catalyst.

Compared with the Sb-containing MoVTe(Sb)NbO<sub>x</sub> catalysts, the Te-containing catalysts are unstable under severe operating conditions [21,45,67], which is mainly due to the sublimation of Te elements in the orthorhombic structure of M1 to form inactive MoO<sub>2</sub> phase [45], which limits the operating temperature of Te containing M1 catalysts (<500 °C) and feed compositions, as shown in Figure 5. Nevertheless, among the orthorhombic structure of Mo-V-based catalysts, the quaternary Mo-V-Nb-Te-O<sub>x</sub> mixed metal oxide has the most excellent catalytic performance in the ODHE process [54,65,68–71].

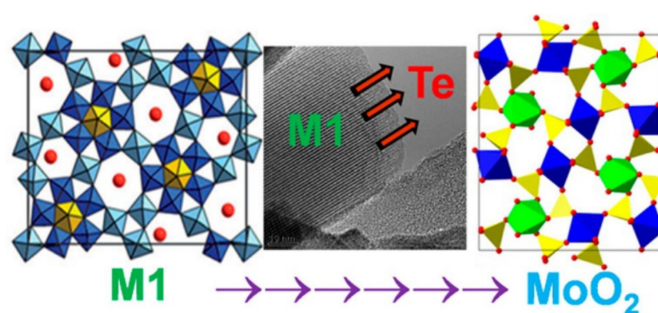


**Figure 5.** Te sublimation from the M1 phase under severe reaction conditions converts to the MoO<sub>2</sub> phase. Adapted from ref. [45], Copyright (2014), with permission from the American Chemical Society.

As a quaternary composite metal oxide, the MoVNbTeO<sub>x</sub> oxide can be formed with varied compositions [72] (Figure 6). Naraschewski et al. [73] suggested that the MoVNbTeO<sub>x</sub> exists mainly in the M1 phase when it is in the bulk composition range of MoV<sub>0.14–0.22</sub>Te<sub>0.1–0.2</sub>Nb<sub>0.1–0.2</sub>O<sub>x</sub>.

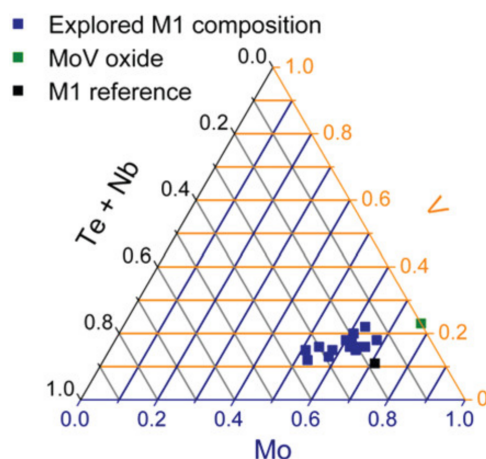


**Figure 6.** Metal stoichiometry (at. %) of M1 catalysts prepared by different methods. The Te- and Nb-free MoV oxide with orthorhombic structure was prepared for reference. Adapted from ref. [72], Copyright (2010), with permission from the American Chemical Society.

As shown in Figure 7, the M1 is an orthorhombic structure, and the *ab* planes are stacked along the [001] direction. The structure is composed of a network of  $\text{MO}_6$  ( $M = \text{Mo}, \text{V}$ ) octahedra, forming pentagonal, hexagonal, and heptagonal channels. This particular phase has several mixed Mo/V sites. It is believed that the location and occupancy of Mo/V sites play a critical role in determining catalyst mechanisms and performance [74]. Moreover, Nb occupies the center of the pentagonal channel and is surrounded by the five  $\text{MO}_6$  ( $M = \text{Mo}$  or  $\text{V}$ ) octahedra, and one of the octahedra contains both Mo and V, and the other four contain only  $\text{Mo}^{6+}$  [75,76]. The hexagonal and heptagonal channels are partially occupied by finite  $(\text{TeO})_n$  zigzag chains [76,77]. Typically, the  $\text{V}^{5+}$  sites in the (001) plane seem to be the active sites in this phase, which are spatially separated from each other by the  $\text{Nb}^{5+}$  bipyramids. The introduced tellurium not only has a role in the catalyst structure but also acts as a bulk component responsible for the storage of oxygen in the hexagonal channel [78], which acts as an oxygen reservoir in the catalytic redox process.

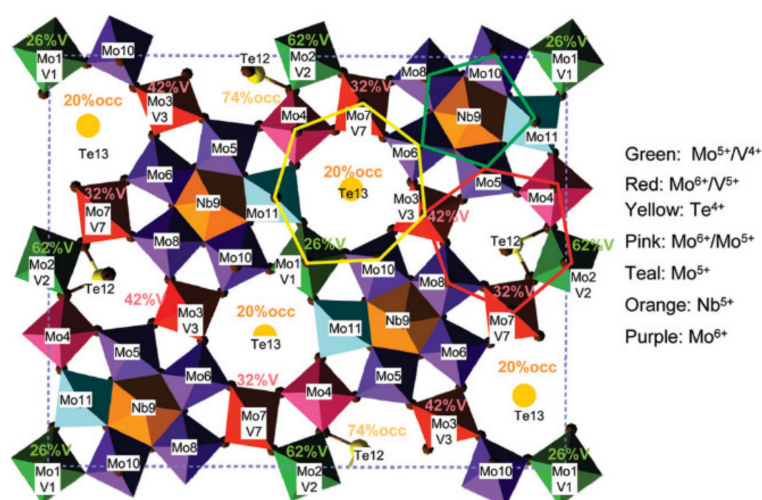


**Figure 7.** The rendering of the model M1 structure from simultaneously refined powder X-ray and neutron data. Adapted from ref. [76], Copyright (2008), with permission from the American Chemical Society.

## 2.2. Mechanism of M1 in the ODHE Process

### 2.2.1. Nature of the Active Sites

As mentioned above, the ODHE over M1  $\text{MoVNbTeO}_x$  catalysts follows the  $\text{MvK}$  redox mechanism, in which the cleavage of the C-H bond in ethane is the rate-determining step [79]. As shown in Figure 8, the M1 is a rod-like crystal with an orthorhombic structure whose long axis coincides with the *c* direction. The basal *ab* planes are perpendicular to the *c*-axis, which means the fast growth in the (001) direction may possess the highest surface energy [48]. Although there remain some conflicts, the current works generally agree that the basal surface is the active surface where the cleavage of the C-H bond occurs. The selective oxidative of light alkanes over M1 phase catalysts is a surface reaction, where the  $\text{V}^{5+}$  in close vicinity to  $\text{Te}^{4+}$  oxo-sites in the basal plane acts as the active site for the activation of light alkanes [14]. A variety of works have demonstrated that the bulk of the M1 phase acts as a structurally stable carrier, which enables the formation of a thin active surface layer [14,80], having an elemental composition different from that of the surface [81]. The presence of a large number of alkane adsorption sites on the surface of the catalyst corresponds to an approximate monolayer coverage [14]. The catalyst surface is a dynamic structure, and the surface is re-structured under reaction conditions [14,82].

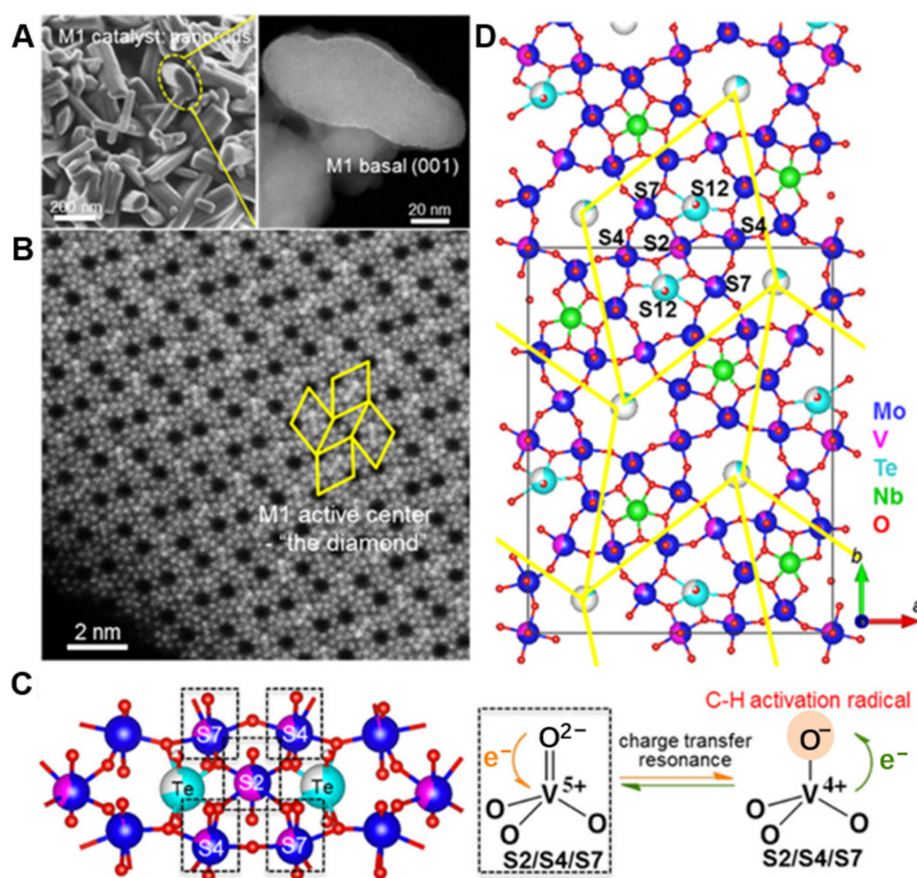


**Figure 8.** (A) SEM image of rod-like Te-M1 catalysts and STEM overview of its (001) basal plane. (B) High-resolution low-angle annular dark field STEM image of proposed active centers (S2–S4–S7 in the yellow-diamonds). (C) Atomic model of the Te-M1 phase (unit cell in black frame). (D) Scheme of the proposed V=O active site on Te-M1. Adapted from ref. [83], Copyright (2017), with permission from the American Chemical Society.

Over the past decade, an increasing number of efforts have focused on the exploration of catalytic active sites of the M1 phase. Nevertheless, the determination of the active site of the catalyst is still controversial. The selective oxidation of light alkanes taking place in M1 catalysts is a surface reaction; therefore, many researchers have investigated the role of different facets of the M1 phase. Celaya Sanfiz et al. [15] have investigated the role of the (001) plane in M1 MoVNbTeO<sub>x</sub> in the selective oxidation of propane to acrylic acid by preferentially exposing this surface. The results suggested that the exposed (001) plane does not have better activity compared with the lateral in the process of propane oxidation. Kolen'ko et al. [13] have synthesized a series of MoVTeNbO<sub>x</sub> catalysts with different dimensions and morphologies. The catalytic performance of catalysts in the selective oxidation of propane to acrylic acid showed that the active site appeared over the entire M1 surface and that the catalyst performance was highly sensitive to the synthesis procedure. Chu et al. [17] used oxalic acid treatment to modulate the morphology of M1 catalysts and investigated its structure sensitivity during the ODHE process. Oxalic acid retained the anisotropic growth of the basal plane during the calcination and obtained smaller M1 needle diameters with promoted surface area. The catalyst activity was optimized at an oxalic acid concentration of 1.0 mmol/L. This work demonstrated that the catalytic performance of the M1 phase is affected by not only the specific surface area but also the aspect ratio of the particle. The lateral surface also possesses active vanadium sites which can convert ethane but mainly correspond to non-selective sites. They suggested that the use of a phase-pure M1 catalyst with a lower aspect ratio in the ODHE process would be more favorable for ethylene selectivity. Melzer et al. [16] have synthesized the

M1 phase with equal chemical composition and different morphologies (Figure 9). They found that facets (010), (120), and (210) are the most frequent lateral termination planes in the M1 phase. The activity in the ODHE process of M1 was normalized to different facets, and it was quantitatively demonstrated that the difference in catalytic activity between M1 samples with the same chemical composition depends mainly on the morphology of the particles, which determines the main termination facets. Then, they synthesized catalysts with a high specific surface area and (001) surface exposure ratio by an improved hydrothermal synthesis method [84].

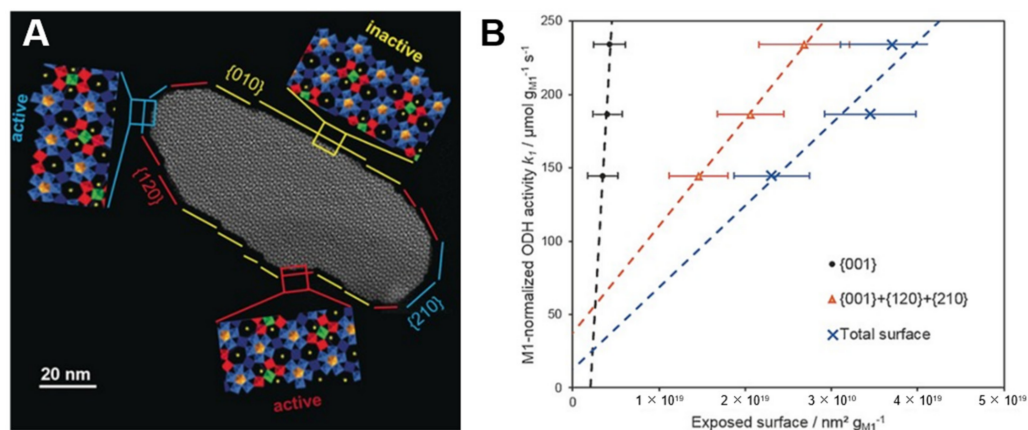


**Figure 9.** (A) Unprocessed STEM image showing crystalline lateral termination facets of a typical flattened M1 particle viewed along [001] direction. (B) Comparison of activity for basal plane (001) with the combination of active facets and with the total surface area. Adapted from ref. [16], Copyright (2016), with permission from John Wiley & Sons.

Chen et al. [18] applied a gentle machinal water agitation method to break up the M1 particles to obtain a series of M1 catalysts with different specific surface areas, particle sizes, and aspect ratios without damage to the microstructure of the catalyst. As shown in Figure 10, the particle size and aspect ratio are reduced after the water mixing treatment, which means a higher proportion and amount of basal surface. The ethane consumption rate is strongly proportional to the amounts of basal surfaces, while the intrinsic selectivity is correlated with the aspect ratio. This evidence suggests that the ODHE process occurring in the M1 phase takes place mainly on the basal surface of the M1 catalyst. In addition, some active sites are also present on the lateral surfaces but are mainly responsible for non-selective oxidation reactions.

The amount and form of oxygen species are important properties of M1 that affect the activity of the M1 catalyst and the selectivity of the product during ODHE. It was suggested that strongly bonded lattice oxygen with nucleophilic properties is responsible for selective oxidation, while weakly bonded reactive oxygen with electrophilic properties contributes to complete oxidation [85]. Sadovskaya et al. [86] used the isotopic oxygen exchange method to investigate the forms of surface oxygen species of MoVNbTeO<sub>x</sub> mixed oxides. There are two forms of exchangeable oxygen on the surface, strongly bonded lattice oxygen species (nucleophilic oxygen) corresponding mainly to selective oxidation to form ethylene and weakly bonded adsorbed oxygen species (electrophilic oxygen) leading to the formation of overoxidized carbon oxides.

Moreover, the hexagonal and heptagonal pores on (001) form channels along the *c*-axis, as shown in Figure 11. Sadakane et al. [87] have reported a novel Mo–V oxide octahedral molecular sieve with an orthorhombic structure, which possesses microchannels composed of seven-membered rings. They demonstrated that the diameter of the channel is about 0.4 nm which is similar to the kinetic diameter of ethane molecular, and the structure has reversible redox properties. Over the past few years, Ueda's group [49,87–90] and Deshlahra's group [91–94] have carried out extensive research works on the micropores

of the M1 phase, which led to a deeper understanding of the nature of the active site of orthorhombic M1 phase at the molecular level.

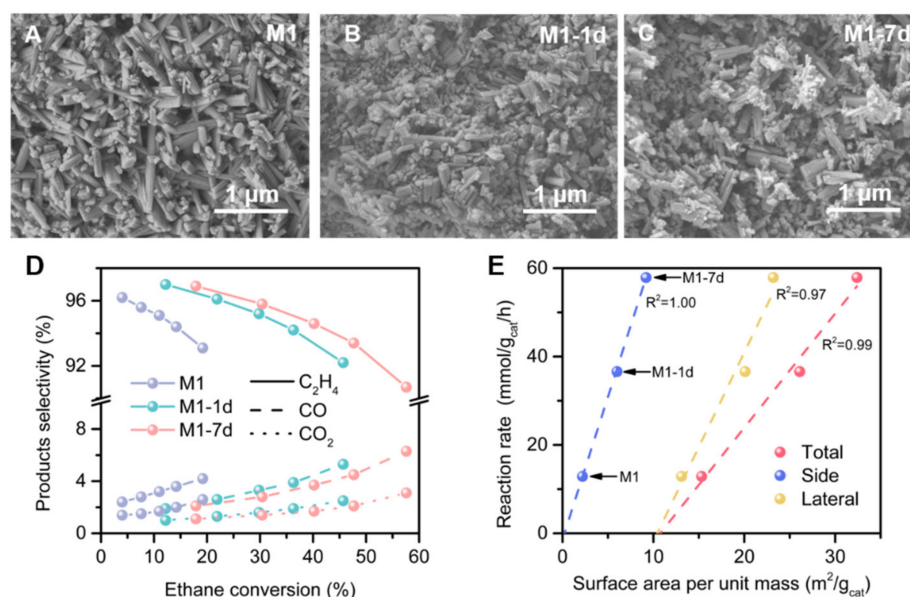


**Figure 10.** M1 catalysts with different specific surface areas, particle sizes, and aspect ratios after water agitation treatment for several days (A–E). Adapted from ref. [18], Copyright (2022), with permission from Elsevier.

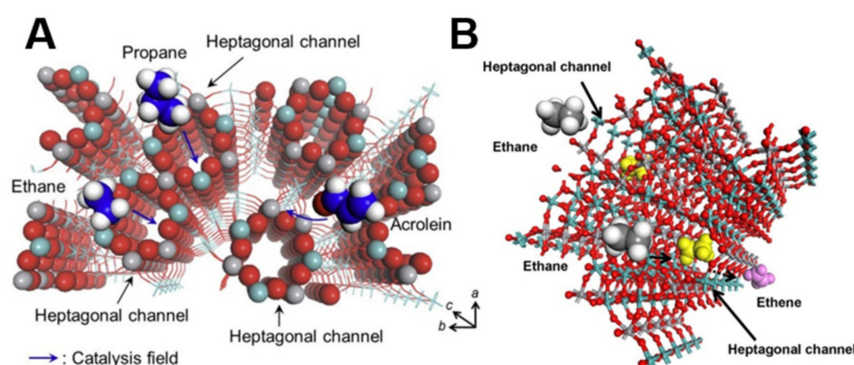


**Figure 11.** The heptagonal channel in the MoV catalysts for the selective oxidation of light alkanes. (A) Propane and (B) Ethane. Adapted from refs. [88,90], Copyright (2014), with permission from Elsevier.

Ishikawa et al. [88,90] have synthesized a series of orthorhombic Mo<sub>3</sub>VO<sub>x</sub> oxide catalysts with the same micropore volumes and varieties of particle sizes and different external surface areas by hydrothermal method. They proposed that heptagonal channels are responsible for catalyzing ethane, propane, and acrolein, while the catalytic fields are different for molecules with different sizes and functional groups. The ethane is small enough compared to the heptagonal pore so that it can enter the heptagonal channel and be converted to ethylene. Subsequently, they treated the orthorhombic structure MoVO catalysts with redox treatment and investigated its crystal structure, microporosity, and catalytic activity [89]. During the reduction treatment process, there are two types of oxygen involved,  $\alpha$ -oxygen and  $\beta$ -oxygen. In the first stage, the release of  $\alpha$ -oxygen from the structure caused an enlargement of the heptagonal pores accompanied by an increase in the conversion of ethane. With further reduction,  $\beta$ -oxygen was extracted from the MoO<sub>6</sub> unit, causing the unit to move toward the microporous channel, thus reducing the pore size, accompanied by a decrease in the conversion of ethane. This strong correlation also confirms

once again that the heptagonal channel in the orthorhombic MoVO<sub>x</sub> phase is the active site for the ethane conversion. Annamalai et al. [92] have investigated the role of heptagonal channel micropores of the M1 MoVNbTeO<sub>x</sub> catalysts by using reactant size-dependent kinetic probes and density functional theory. Compared with non-microporous vanadium oxides, the M1 phase showed a high C<sub>6</sub>H<sub>12</sub>/C<sub>2</sub>H<sub>6</sub> rate ratio, suggesting that the C<sub>2</sub>H<sub>6</sub> size and heptagonal micropores show a tight fit, while the C<sub>6</sub>H<sub>12</sub> cannot access intrapore sites. The DFT results show that most of the C<sub>2</sub>H<sub>6</sub> activation occurs inside the micropores, which stabilize the C-H activation transition state via van der Waals interactions. The tight confinement in micropores hinders the C-O contact necessary for O-insertion, thus intrinsically ensuring high selectivity of ethylene.

In situ characterization techniques are a powerful tool to probe the catalyst properties under reaction conditions. In the last decade, much effort has been made in situ characterization to reveal the catalyst properties under reaction conditions [14,62,82,95–100] (listed in Table 1). As mentioned above, MoVNbTeO<sub>x</sub> catalysts were previously used for the selective oxidation of propane/propylene, so that most of the in situ characterization research work is based on the propane/propylene reaction. Nevertheless, it is still of some reference values. Aouine et al. [62] used in situ environmental STEM to characterize the surface properties of the M1 phase during the selective oxidation of ethane under different atmospheres. Under the reaction conditions, the structure of the M1 MoVTeO<sub>x</sub> catalyst remained stable without any disorder. Furthermore, the results showed that the Te-O<sub>x</sub> chains in the hexagonal channels were involved in the redox of the catalyst and the re-oxidation of the active sites on the surface, which proved the role of the hexagonal channels as oxygen reservoirs in the ODHE process. Under reducing conditions, the removal of labile oxygen leads to the reduction of Te elements and, thus, to a high degree of freedom, which is responsible for the partial volatilization of Te at the surface. Hävecker et al. [14] used in situ photoelectron spectroscopy technique to probe the surface information of MoVNbTeO<sub>x</sub> during the reaction conditions. It was confirmed that the surface composition of M1 differs significantly from that of the bulk, implying that the active sites on the surface are not part of the M1 phase. The exposure of the inner surface of the hexagonal and heptagonal channels on the laterally terminated M1 phase provided an explanation for the difference in chemical composition and the existence of potential active ensembles on the entire M1 surface. Under the reaction conditions, the products formed were associated with a decrease in Mo<sup>6+</sup> and an increase in V<sup>5+</sup> sites, while only vanadium showed a dynamic change in the valence state. They proposed that the bulk of the M1 phase is a structurally stable carrier, allowing it to form a thin active surface layer that contains active V<sup>5+</sup> sites in close vicinity to the Te<sup>4+</sup> oxo-sites.

**Table 1.** Summary of the in situ techniques used for MoVNbTeO<sub>x</sub> catalysts.

Technique	Ref.
STEM	[62]
(NAP) XPS	[14,96,97,99,101]
NEXAFS	[101]
XRD	[66,97,99]
Raman	[95]
FTIR	[95]

Over the past years, many kinetic models have been applied to describe the reaction mechanism of ODHE based on vanadium and M1 MoVNbTeO<sub>x</sub> catalysts. Especially the development of computer computing power has made it possible to understand complex MoVNbTeO<sub>x</sub> catalysts based on density functional theory (DFT) at the molecular level. Cheng et al. [102,103] used DFT to determine the reaction mechanism for the activation of propane in the M1 phase of MoVNbTeO catalysts. They found that the C-H bond is activated by the Te=O sites coupled to the V=O centers through a reduction-coupled oxidative activation mechanism, in contrast to the previous suggestions for vanadium and molybdenum oxides that oxygen bond directly to V or Mo is responsible for the activation of the initial

alkane C-H. The ability of the T=O to activate the C-H bond in alkane depends sensitively upon the number of V atoms that are coupled through a bridging O to the Te=O center.

Liu et al. [93] used DFT calculations to demonstrate the reaction pathways of the ODHE process (see Figure 12). Reaction paths based on the selective oxidation of ethane to ethylene and the non-selective oxidation to carbon oxides through the consecutive-parallel pathway with different environmental O atoms were probed. The results show that the higher intrinsic ethylene selectivity mainly originates from the heptagonal pores located on the (001) plane and not from the (001) surfaces. The C-H activations and C-O bond formations leading to C<sub>2</sub>H<sub>4</sub> and oxygenates, respectively, prefer to involve terminal O atoms on (001) surfaces.

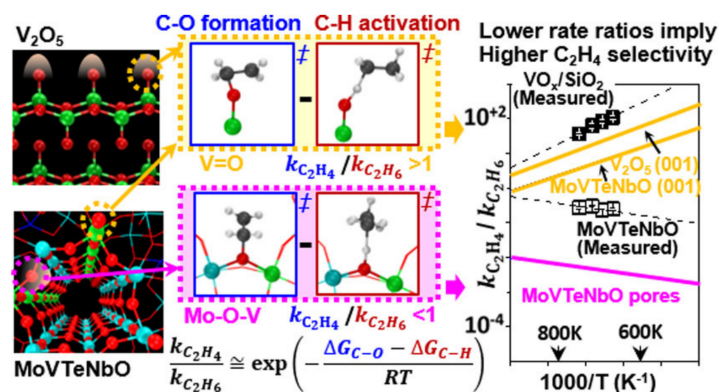


**Figure 12.** Effects of lattice O atom coordination and pore confinement on selectivity limitations for the ODHE process. Adapted from ref. [93], Copyright (2019), with permission from the American Chemical Society.

Qian et al. [29] investigated the active sites of phase-pure M1 MoVNbTeO<sub>x</sub> catalysts for the ODHE reaction using an atomic substitution strategy (see Figure 13). Density of states and crystal orbital Hamiltonian population (COHP) calculations indicate that the adsorption of H atoms will weaken the strength of the transition metal-oxygen bond. The integrated COHP and Bader charge are useful descriptors to correlate the electronic structure to the catalytic performance of M1 MoVNbTeO<sub>x</sub> catalysts. The Te-O site located in the M1(001) plane is considered to be an important active site for both ethane conversion and ethylene selectivity. In addition, there is a linear relationship between surface V content and ethane conversion. Therefore, synergistic interaction between the Te-O and V-O sites is considered an intrinsic active site for the ODHE reaction.

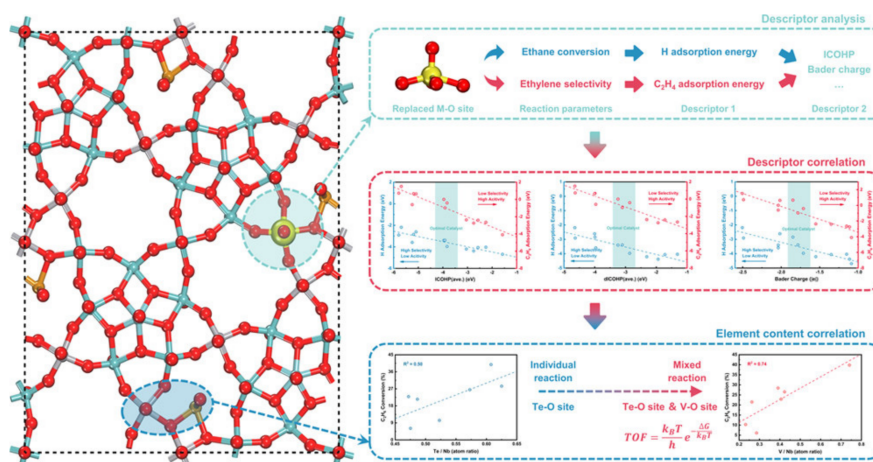


**Figure 13.** The influence of the introduction of different elements in the Mo-V M1 structure in the oxidative dehydrogenation of ethane. Adapted from ref. [29], Copyright (2022), with permission from the American Chemical Society.

### 2.2.2. Kinetic Model for Oxidative Dehydrogenation of Ethane

So far, a number of models have been used to describe the kinetics of the selective dehydrogenation of light alkanes (please refer to a review by Grabowski [104]). Although numerous reaction mechanism models were applied to the description of ODHE over M1 catalysts, these kinetic data consistently indicate that the ethylene formation is the reaction requiring the lowest activation energy, and the rate is weakly affected by changes in oxygen partial pressure [105–107].

As one of the simplest reaction mechanism models, though power law-based kinetics models disregard mechanistic aspects, they are extensively used for reactor scale-up and design. Valente et al. [105] have developed a power-law kinetic model of the M1 catalyst by regressing data obtained by varying the operation conditions (temperature, contact time, feed compositions, etc.), which have been used for the process simulation by Gaffney et al. [108].

Che-Galicia et al. [106] developed a kinetic model of the ODHE process in M1 catalysts based on the Langmuir-Hinshelwood-Hougen-Watson (LHHW), MvK, and combined form mechanisms. The LHHW mechanism showed the best agreement with the experimental data in terms of statistical results, where the adsorbed water on the active sites affects the reaction rates negatively. Nevertheless, more work has demonstrated that the ODHE process over the M1 catalyst should be more in accordance with the MvK mechanism [79,109], which is first-order dependence on the ethane and zero-order for oxygen [18,110,111]. The lattice oxygen species of the catalyst are responsible for cleaving the C-H bonds in ethane, and they are re-oxidized by the gaseous oxygen species to replenish the consumed lattice oxygen.

Donaubauer et al. [107] proposed an MvK-like mechanism for the ODHE reaction on the M1 catalyst, as shown in Figure 14. They classified the surface oxygen species of the catalyst into two different oxygen sites, that is, the lattice oxygen species responsible for cleaving the C-H bond in ethane and the electrophilic surface oxygen species responsible for inserting O atoms to form C-O bonds. Sensitivity analysis shows that the rate of ethylene formation is strongly influenced by the initial cleavage of the C-H bond in ethane, and the replenishment of lattice oxygen species will be limited under low oxygen operating conditions, leading to a constrained redox cycle.

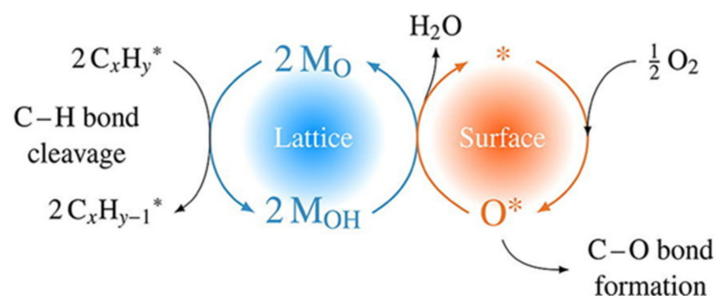


**Figure 14.** The catalytic cycle for the ODHE reaction on MoVTeNb mixed metal oxides proposed by Donaubaauer et al. Adapted from ref. [107], Copyright (2020), with permission from Elsevier.

## 3. Catalytic Performance of MoVNbTeO<sub>x</sub> for ODHE

### 3.1. Catalyst Activity and the Ways to Improve

A great deal of work has been carried out to improve the activity of M1 catalysts. Optimization of synthesis procedures, doping with other elements, the introduction of other phases, etc., have been employed.

#### 3.1.1. Doping Method

The introduction of new elements as promoters in the catalyst system seems to be a useful way to modulate the catalytic performance. For MoVTeNb multi-component oxides, a lot of work has been investigated in elemental doping methods, including Cu, Fe, Sm, Sn,

Bi, Co, Cr, Ce, Bi, In, Ni, Mn, Ga, K, Bi, and Ge, etc. [112–116], and some of these catalysts were evaluated in the ODHE.

Ishchenko et al. [114,116] investigated the effect of Bi and K doped M1 MoVTeNbO<sub>x</sub> catalysts on the catalytic performance of ODHE to ethylene. The introduced K and Bi are well dispersed on the M1 phase and become part of the M1 phase without the presence of any corresponding compound. These two additives show different effects on the M1 phase, including morphology, structure, valence state of surface V and Mo elements, and surface abundance of Te, giving opposite results on the catalyst activity. The additive of K into the M1 phase promotes the growth of the particles along the (001) direction, while the additive of Bi into the M1 phase does not affect the morphology of the M1 phase but modifies the structural features with an increased proportion of accessible (001) surfaces. The doped K decreases the active surface and abundance for both V<sup>5+</sup> active sites and Te on the surface, while Bi-doped samples show a different trend with a positive effect on the catalytic performance. Furthermore, the effect of Bi concentration in the MoVNbTeO<sub>x</sub> M1 phase was investigated for selective ODHE. A strong correlation between the concentration of Bi and properties of the prepared catalysts was observed. An optimized concentration of Bi can have the modified MoVNbTeO<sub>x</sub> catalysts with the best catalytic performance, ethylene selectivity, and stability. The doped Bi can constrain the Te segregated from the hexagonal channel to prevent the loss of Te so as to improve the stability of the M1 phase during ODHE.

Yun et al. [115] prepared MoVTeNb(Ce)O catalysts using Ce as a promoter doped into M1 in the framework. The doping of Ce promotes the reducibility of the M1 phase and increases the amounts of active sites and lattice oxygen species available for ethane conversion. As shown in Figure 15, the improved properties significantly enhanced catalytic performance and maintained excellent ethylene selectivity. Lazareva et al. [117] used Nd, Mn, Ga, and Ge as promoters to modify the catalytic properties of MoVNbTeO<sub>x</sub> catalysts, which seems to be inserted into the orthorhombic structure. The physical-chemical properties of MoVNbTeO<sub>x</sub> were affected, including the content of the M1 phase, surface compositions, and acidities. At small amounts of additives, the catalytic performance was enhanced during the ODHE process. The introduced elements were well dispersed on the M1 phase, and the valence of all elements and the composition of the surface M1 catalyst were comparable to those of the unmodified sample. Moreover, the ethylene over-oxidation at high ethane conversion was suppressed by the reduced amount of acid sites, which positively influenced the M1 catalysts with a high intrinsic ethylene selectivity.

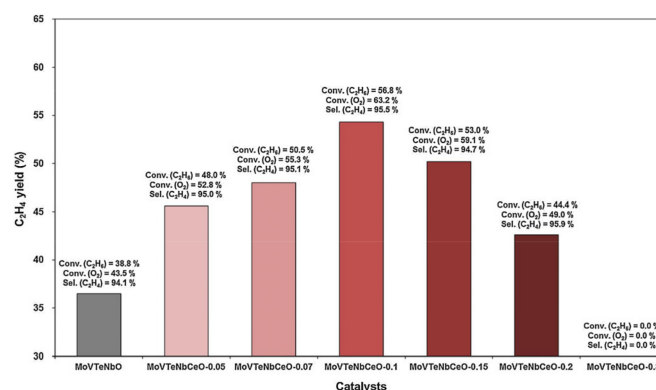


**Figure 15.** Catalytic performance of Ce-doped MoVTeNb(Ce)O catalyst with various Ce contents. Adapted from ref. [115], Copyright (2018), with permission from Elsevier.

### 3.1.2. Post Treatment Method

Chu et al. [21] investigated the catalytic performance of the MoVTeNbO<sub>x</sub> catalyst in ODHE, which was prepared from the same precursor slurry by hydrothermal synthesis with different post-treatments. The different purification processes will affect the tellurium contents and V<sup>5+</sup> concentration in the catalysts. They proposed that the catalytic perfor-

mance is directly related to the amount of  $V^{5+}$ . While the formation of reduced Te blocks the active site, which is considered to be the main reason for catalyst deactivation. Therefore, lower Te content will facilitate the formation of stable catalysts and reduces the risk of Te aggregation. The hydrogen peroxide treatment will increase the  $V^{5+}$  concentration and decrease the Te content, which can simultaneously improve the catalytic activity and stability of the catalysts in the ODHE process. However, under severe operating conditions, the phase-pure M1 catalyst with low Te content can also be significantly deactivated due to the conversion of the active phase to the inactive phases. Although the surface morphology of the oxalic acid-treated M1 phase was improved with a significant reduction in particle size and an increase in surface area, the loss of vanadium during the treatment reduced its catalytic activity.

The non-thermal plasma consists of energetic components that can modify the surface by a physical or chemical interaction of the active species in the gas phase with the solid surface shown in Figure 16. Chen et al. [19] used oxygen plasma with strong oxidization properties to modify the surface of the M1 phase, which can change the valence state of surface vanadium sites to enhance the abundance of active sites. The oxygen plasma can efficiently increase the  $V^{5+}/V^{4+}$  ratio on the catalyst's surface and maintain the structure. The catalytic performance of M1 showed a good correlation with the concentrations of  $V^{5+}$ , which proves the feasibility of this method. Qian et al. [30] also applied this method to modify the M1-CeO<sub>2</sub> nano-composite catalysts, showing a good catalytic performance during the ODHE process.

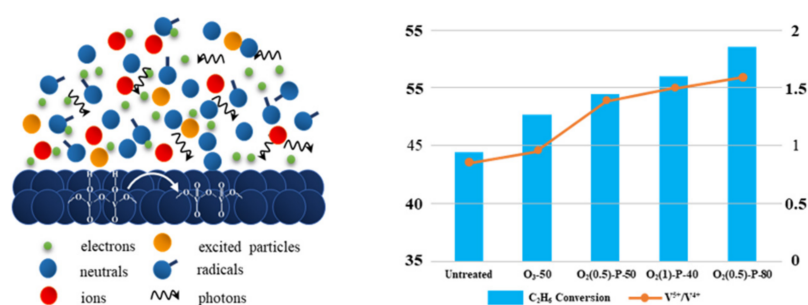


**Figure 16.** The variation of the abundance  $V^{5+}$  content of MoVNbTeO<sub>x</sub> catalysts by non-thermal plasma treatment was correlated with the catalytic performance. Adapted from ref. [19], Copyright (2015), with permission from the Royal Society of Chemistry.

### 3.1.3. Introduction of Diluters/Promoters

Low activity and high catalyst cost are the main issues limiting the application of M1 catalysts for ODHE. Although a number of oxides have been applied to the ODHE process, none of them possess high ethylene selectivity activity except for MoVO<sub>x</sub>, V<sub>2</sub>O<sub>5</sub>, and NiO-based catalysts [23,110,118,119]. However, some oxides exhibit unique redox properties, oxygen storage capacity, and high specific surface area and are often introduced as new phases to improve the catalytic and physicochemical properties of the original catalyst. As for the ODHE process over M1 MoVNbTeO<sub>x</sub> catalysts, much work has been done to introduce oxides phase with poor activity in the ODHE into the MoV-based system to improve the M1 catalytic performance.

Nguyen et al. [70] prepared silica diluted MoVTe(Sb)NbO catalysts by using a slurry method to optimize the catalytic performance during the ODHE process. They investigated the influence of the addition of silica in the slurry solution and the heat treatment in nitrogen after the dissolution of the M2 phase. However, the results showed opposite trends. The introduction of SiO<sub>2</sub> only improved the conversion of ethane without modifying the selectivity of ethylene. In contrast, the re-heat treatment reduced the catalytic performance and improved the selectivity of ethylene. These changes in catalytic properties can be attributed to the same factors, the degree of aggregation and sintering of the M1 phase and the distribution of small pores in the catalyst. Chu et al. [20] used two methods

(sol-gel method and physical mixing method) to combine the  $\text{CeO}_2$  with the M1 phase and form an M1- $\text{CeO}_2$  nano-composite catalyst. The introduced  $\text{CeO}_2$  oxide enhances the catalytic activity of M1 in the ODHE process. Compared with physically mixed M1- $\text{CeO}_2$  nanocomposites, M1- $\text{CeO}_2$  prepared by sol-gel method exhibited smaller  $\text{CeO}_2$  particle size, well dispersed on the surface of the M1 phase, and showed good catalytic properties. In the ODHE process, the introduced  $\text{CeO}_2$  phase enhances the redox properties of M1 phase, and at the same time, the introduced  $\text{CeO}_2$  also enhances the valence state of V, which is related to the particle size of  $\text{CeO}_2$ . As shown in Figure 17, Dang et al. [23] have systematically synthesized a series of M1- $\text{CeO}_2$  nano-composite catalysts by sol-gel method and determined the optimal  $\text{CeO}_2$  loading of 30 wt.%. The results show that the introduced  $\text{CeO}_2$  phase can promote the amounts of active sites, which is one of the major factors affecting the catalytic performance. In addition, the presence of  $\text{Ce}^{4+}$  promotes re-oxidation of vanadium sites, which leads to an increase in the turn-over frequency (TOF). Chen et al. [24] used  $\text{MnO}_x$  oxide as a promoter in combination with phase-pure M1  $\text{MoVNbTeO}_x$  oxide for ODHE. The introduced manganese oxide was used as an oxygen promoter to allow M1 to be oxidized by gas-phase oxygen at a lower temperature during the preparation. In the ODHE process at 400 °C, the promoted M1 catalyst achieved more than 20% catalytic performance based on ethane conversion. Due to the high surface area and redox properties of anatase  $\text{TiO}_2$ , Dang et al. [25,28] used  $\text{TiO}_2$  as a promoter to improve the catalytic performance of the M1 phase during the ODHE process. M1- $\text{TiO}_2$  nano-composites were prepared by the physical mixing method and the sol-gel method. The results showed that M1- $\text{TiO}_2$  prepared by sol-gel method shows a smaller  $\text{TiO}_2$  particle size and well dispersed on the M1 surface, which presented an excellent activity for ODHE. In addition, M1- $\text{TiO}_2$  prepared by sol-gel method was optimized with an optimal  $\text{TiO}_2$  content of 40 wt.%. Although the abundance of  $\text{V}^{5+}$  sites content was enhanced to a certain extent, the total amount of active sites normalized to per mass was decreased after the introduction of  $\text{TiO}_2$ . The improvement in catalytic performance was mainly due to the introduction of  $\text{TiO}_2$  to enhance the reduction/re-oxidation rate of lattice oxygen species in the catalyst.

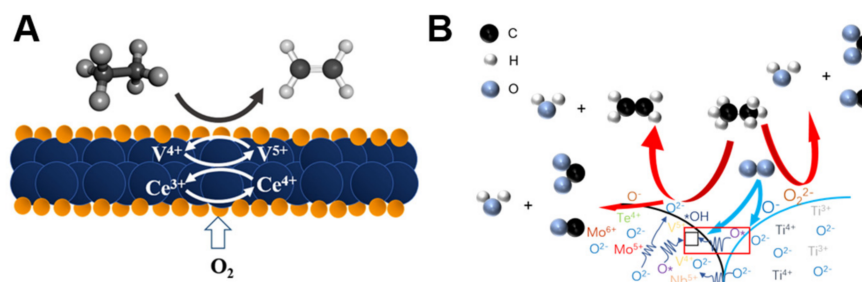


**Figure 17.** (A) The combination of M1  $\text{MoVNbTeO}_x$  with  $\text{CeO}_2$ . (B) M1  $\text{MoVNbTeO}_x/\text{TiO}_2$  nano-composite catalysts with an effect on enhancing the redox properties during the ODHE process. Adapted from ref. [23,28], Copyright (2018), (2022), with permission from Elsevier and Royal Society of Chemistry.

Due to the disadvantages of Te-containing catalysts, which are toxic and harmful to the environment and tend to volatilize during the ODHE reaction, Zenkovets et al. [120] used Ce-doped  $\text{MoVSbNbO}_x$  catalyst with  $\text{SiO}_2$  as diluter to obtain the  $\text{MoVSbNbCeO}_x\text{-SiO}_2$  catalyst by spray drying method in aqueous solution and calcined in He flow. The intergrowth between the M1 and M2 phases in the  $\text{MoVSbNbCeO}_x\text{-SiO}_2$  catalyst forms the interphase boundary of the highly active catalyst. The prepared catalysts can obtain up to 74% ethylene yield, which is the highest ethylene yield reported in the literature for Sb-containing catalysts. López-Medina et al. [121] used alumina as support to deposit the active  $\text{MoVNbTeO}_x$  phase. Compared to their bulk form, the stable nanoscale active  $\text{MoVNbTeO}_x$  can expose a higher active surface and exhibit economic advantages. In

addition, the alumina carrier offers better mechanical resistance and easier control of catalyst pellets formation.

### 3.1.4. Design and Optimization of Synthesis Procedure

Melzer et al. [84] improved the hydrothermal synthesis method by using insoluble metal oxides as raw materials and organic additives, which can generate M1 phases with high surface area, showing higher activity compared to conventionally prepared catalysts. With the help of complexing agents that control the activity of ionic intermediates, the concentration of metal cations and polyoxometalate clusters is controlled at a concentration suitable for crystallization to avoid the formation of amorphous mixed oxides. The excellent catalytic performance can be attributed to the formation of M1 crystals with highly corrugated sidewalls, exposing a large number of active sites (see Figure 18). The proposed synthesis method uses inexpensive and abundant metal oxide reactants and the simplicity of one-batch synthesis, enabling the synthesis can be scale-up directly.

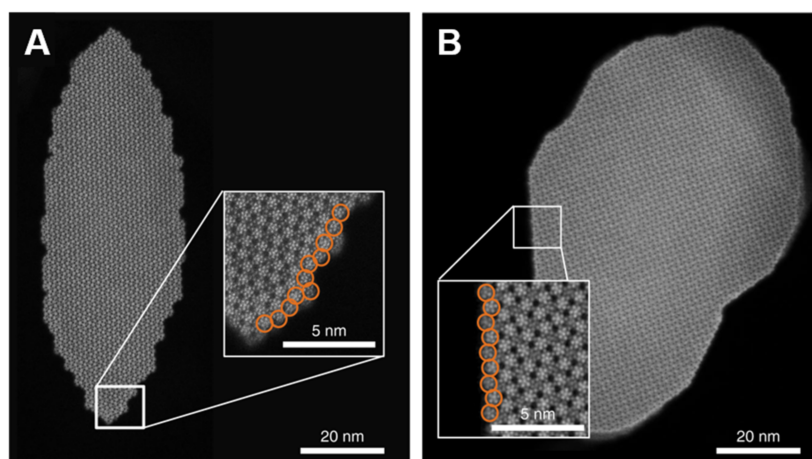


**Figure 18.** ADF-STEM images of the (001) plane of M1 MoVTeNbO<sub>x</sub> particles. (A) Sample prepared by the new synthesis method, after drying overnight in air at 80 °C, and (B) sample prepared by the previous method, followed by crystallization at 650 °C in inert. Insets show representative lateral surface termination. Circles highlight complete pentagonal M<sub>6</sub>O<sub>21</sub> units observed near the termination. Adapted from ref. [84], Copyright (2019), with permission from Springer Nature.

López Nieto's group [122,123] developed a new reflux synthesis method for the preparation of MoVTeNbO<sub>x</sub> metal oxide catalysts, shown in Figure 19. The synthesis procedure and parameters were optimized to obtain catalysts that can compete with conventional preparation methods. The ramp of the synthesis temperature is an important parameter that affects the vanadium content of the precipitate in favor of the formation of a pseudoamorphous Mo-V-Te-Nb oxometallate. The optimized synthesis parameters can produce a MoVTeNbO<sub>x</sub> catalyst with a smaller size, which significantly enhances the catalytic behavior. Yu's group [124–126] investigated the effect of high pressure and temperature on the preparation of MoVNbTeO<sub>x</sub> catalysts in a hydrothermal synthesis method. The catalytic performance of the oxidative conversion of propane/propylene to acrylic acid reaction was investigated. Li et al. [126] synthesized the MoVTeNbO<sub>x</sub> mixed metal oxides in sub/super-critical conditions by a stainless tube-reactor. The synthesized oxides with various phase compositions and morphologies can be directly used to convert propylene to acrylic acid without calcination. The physical-chemical properties are affected by the synthesis temperatures. High temperatures are beneficial for a mixed phase. Moreover, they also have prepared a series of MoVTeNbO<sub>x</sub>-mixed metal oxides by hydrothermal synthesis under different pressure and temperatures [124]. This work suggested that the MoVTeNbO<sub>x</sub> with a high M1 content can be synthesized under a high-pressure condition and a short time without purification. The time of the high-pressure hydrothermal

preparation procedure is significantly reduced (30–60 min) compared to the conventional hydrothermal process (about 48 h). The prepared M1 catalysts exhibit a superior catalytic performance in the oxidative conversion of propane to acrylic acid, which can attribute to the high surface  $V^{5+}$  abundance and proportion of basal (001) planes. Meanwhile, the catalysts also show an excellent stability in the high operation conditions.

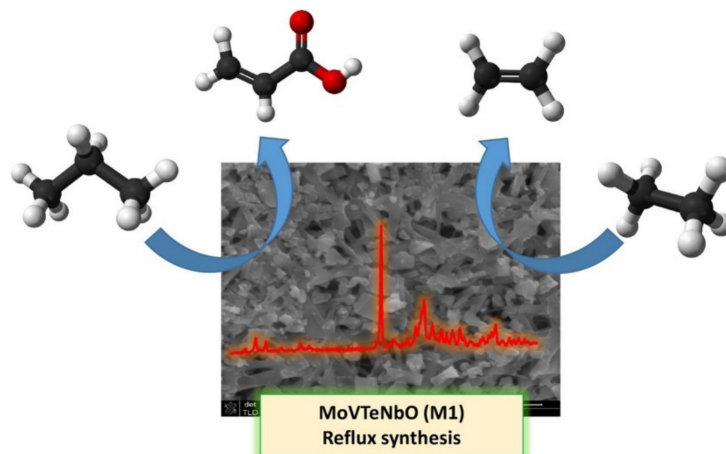


**Figure 19.** Reflux synthesis of the M1 catalyst for the selective oxidation of light alkanes. Adapted from ref. [122], Copyright (2020), with permission from Elsevier.

As a complex catalytic system, the introduction of high-throughput equipment can greatly accelerate the development and optimization process of the  $MoVNbTeO_x$  catalyst [112,127–129]. Mestl et al. [112] used combinatorial and high-throughput methods to investigate the MoVTeNb based catalysts for the oxidation of propane to acrylic acid. The M1 catalysts containing additional promoters (Mn, Ni, W, In, Cu, Sb, Fe, Sm, Sn, Bi, Co, and Cr) were investigated. Moreover, the use of different ratios of citric acid as a structure-directing agent in the synthesis has also been investigated. During the optimization process, a five-generation catalyst was designed by an optimization platform consisting of artificial neural networks and a holographic optimization algorithm. Zhu et al. [129] optimized the MoVNb mixed oxides catalysts for the ODHE process based on a commercial high-throughput reactor system. They screened about 75 catalysts with different Nb loading and Mo/ratio, and a composition range were established based on the high-throughput results.

### 3.2. Reactor Development and Industrial-Scale Tests for ODHE

As shown in Table 2, the exothermic properties of the ODHE process tend to cause hot spots in the reactor, which would lead to temperature runaway in the reactor so as to negatively affect the product selectivity distribution and stable reactor operation. Over the years of research, some attempts have been carried out to apply ethane oxidative dehydrogenation on an industrial scale. Dalian Institute of Chemical Physics, Chinese Academy of Sciences and Wison Engineering have been devoted to the industrial development of ODHE to ethylene technology, and the related technology passed the pilot evaluation in 2021, which marks that the catalytic ODHE to ethylene is ready for industrial and commercial implementation [130].

**Table 2.** The ODHE reaction network consists of selective oxidation of ethane to ethylene.

	Reaction	$\Delta_r H^\circ$ (kJ/mol)
Main reaction	$C_2H_6 + 0.5O_2 \rightarrow C_2H_4 + H_2O$	−105
	$C_2H_6 + 3.5O_2 \rightarrow 2CO_2 + 3H_2O$	−1428
Side reactions	$C_2H_6 + 2.5O_2 \rightarrow 2CO + 3H_2O$	−861
	$C_2H_4 + 3O_2 \rightarrow 2CO_2 + 2H_2O$	−1218
	$C_2H_4 + 2O_2 \rightarrow 2CO + 2H_2O$	−652

### 3.2.1. Lab-Scale Reactor Design

As shown in Figure 20, Nguyen et al. [131] have synthesized a structured MoVTenbO<sub>x</sub> supported on pre-oxidized SiC foam by dip coating from slurry containing the precursors as catalysts for the ODHE and the ammoxidation of propane. However, the structured catalysts showed lower activity and ethylene selectivity compared to the powdered form due to the lower content of the M1 phase and the presence of other active but non-selective phases in the structured catalyst.

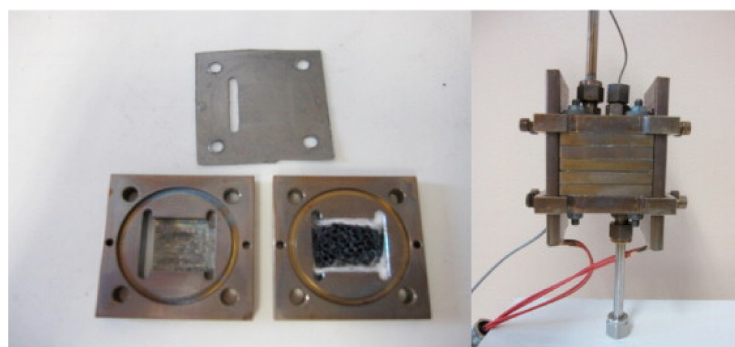


**Figure 20.** Photography of the complete reactor with five platelets with cover plates on each side with, gas entrance and exit, and thermocouple and the morphology of SiC with MoVNbTeO<sub>x</sub> catalyst. Adapted from ref. [131], Copyright (2012), with permission from Elsevier.

As a superior support for structured catalysts in industry implementations, cordierite has good chemical inertness, high thermal stability, and low thermal expansion coefficient. As shown in Figure 21, Chen et al. [27] used cordierite monolith as a carrier to prepare an M1@Cordierite structured catalyst for the strong exothermic properties of the ODHE process. A CeO<sub>2</sub> layer was pre-coated on the cordierite to improve the catalytic performance of the structured catalyst. The M1@CeO<sub>2</sub>@Monolith layered structure prepared by the two-step procedure shows excellent superior catalytic performance and stability for the ODHE reaction. Due to the constrained contact between the gas phase and the CeO<sub>2</sub> interlayer, the formation of CO<sub>x</sub> is inhibited, thus maintaining the selectivity of ethylene. In addition, the structured M1@CeO<sub>2</sub>@Monolith catalyst shows comparable ethylene selectivity to the powdered form diluted by 10 times silicon carbide, and the temperature runaway due to the highly exothermic reaction has been avoided. Yan et al. [31] also used a foam SiC with a high thermal conductivity as a structuring support to coat a crystalline M1 powder catalyst onto this carrier and investigated methods to enhance the stability of the coating layer. The M1@foam SiC structured catalyst shows an excellent heat transfer and catalytic performance, which can eliminate the generation of hot spots and maintain the ethylene selectivity as well. Proper calcination treatment is beneficial to achieve good coating layer adhesion without loss of activity, while the addition of a binding agent, or a “stabilize the coating first, then activate the catalyst strategy, can achieve a robust coating and fair catalytic performance.

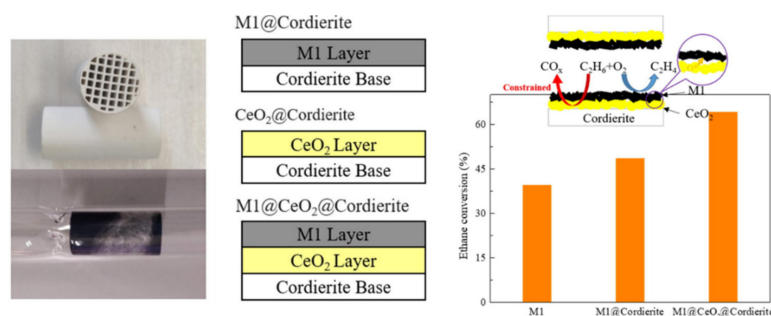


**Figure 21.** Scheme of M1@CeO<sub>2</sub>@Cordierite structured catalyst and catalytic performance for the ODHE process. Adapted from ref. [27], Copyright (2022), with permission from Elsevier.

Chu et al. [22] applied the microreactor to the strongly exothermic ethane oxidative dehydrogenation reaction (see Figure 22). The hot effect during the oxidative dehydrogenation of ethane was investigated in a lab-scale fixed reactor (inner diameter of 8 mm) with different diluter-catalyst ratios. Hot spots in the lab-scale fixed-bed reactor can be eliminated when the ratio of SiC to catalyst is up to 10 times. At a SiC/catalyst ratio of 1/4, the hot spot temperature in the lab-scale fixed bed reactor is about 100 °C higher than that of the reactor environment and causes a significant decrease in ethylene selectivity and catalyst stability. In that work, they used PVA solution as a binder to prepare a stable and active phase-pure M1 catalyst layer on a metal-ceramic composite substrate by dip-coating method and inset into a micro-reactor to avoid the generation of hot spot. Compared with the microchannel reactor, the traditional fixed-bed reactor needs about 5 times its volume to achieve the same reactor productivity. Lin et al. [132] also utilized the merits of the large heat transfer surface area and short heat transfer distance of the micro-reactor to achieve better-controlled operation conditions, especially the reaction temperature during propane ammoxidation over MoVNbTeO<sub>x</sub> catalyst. Compared with the temperature gradient in a conventional fixed bed tubular reactor (43.2 °C), the gradient in a microchannel reactor can be controlled at less than 0.5 °C. The strongly exothermic propane ammoxidation reaction can be easily and precisely operated in a microchannel reactor under much harsher reaction conditions to achieve higher productivity and selectivity.

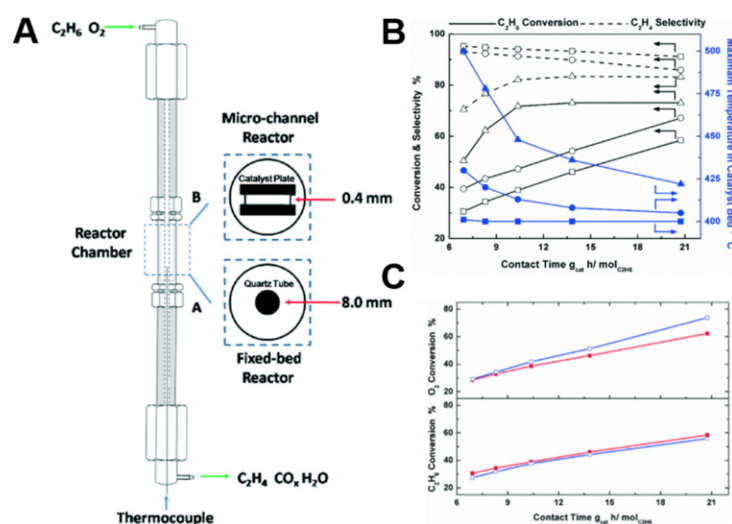


**Figure 22.** (A) Schematic diagram of the fixed-bed reactor and the micro-channel reactor. (B) Ethane conversion, ethylene selectivity, and hot spot temperature in the catalyst bed as functions of contact time for M1 catalyst powder in the fixed-bed reactor. Experiments were performed at 400 °C and 1.0 atm with a C<sub>2</sub>H<sub>6</sub>/O<sub>2</sub>/He molar ratio of 30/20/50 and a diluter-to-M1 catalyst mass ratio of ((<sup>▲</sup>) 1:4, (<sup>●</sup>) 5:1 and (<sup>■</sup>) 10:1 at a reactor inlet. (C) Ethane and oxygen conversion as functions of contact time, M1 catalyst in the fixed-bed reactor (<sup>■</sup>) and in the micro-channel reactor (<sup>□</sup>). Experiments were performed at 400 °C and 1.0 atm with a C<sub>2</sub>H<sub>6</sub>/O<sub>2</sub>/He molar ratio of 30/20/50 at the reactor inlet. Adapted from ref. [22], Copyright (2015), with permission from the Royal Society of Chemistry.

### 3.2.2. Industrial-Scale Reactor Design

Che-Galicia et al. [133] regressed a kinetic model in lab-scale experiments and then coupled it with an industrial-scale reactor transport parameters obtained from other independent experiments. Industrial-scale wall-cooled packed bed reactor models illustrate the importance of transfer parameters for the simulation of this reactor. The coolant will affect the temperature distributions and formation of hot spots in the large-scale packed reactors, which will cause the damage of M1 MoVNbTeO<sub>x</sub> catalysts.

Chen et al. [134] have developed an experimentally based kinetic model over M1 catalyst and applied it for comparison between autothermal and multi-tube reactors and

demonstrated a feasible autothermal reactor design for ODHE (see Figure 23). The results show that the autothermal reactor configuration is more favorable for the high exothermic ODHE process. The highly exothermic properties of the ODHE process makes it hard to be operated steadily in a multi-tubular reactor. Although the diluents for the reactants and catalyst bed will help to reduce the exothermic intensity, this is achieved at the cost of reduced capacity. The designed autothermal reactor with cold feed allows for near-complete conversion of oxygen in the outlet and reduces the size of the reactor by a factor of 2–10. Fazlinezhad et al. [135] investigated the effect of removing water treatment on the ODHE process over  $\text{MoVTenNbO}_x$  catalyst in the fixed-bed reactor. After water removal, the reactor hotspot and temperature were reduced, with the hotspot dropping from 500 °C to 460 °C, making the operation more controllable. Besides, the ethylene was enhanced after the removal of water. Moreover, a 20-bed mode membrane-like reactor was also investigated to remove water more sufficiently, which resulted in more than 94% ethylene selectivity. Therefore, a membrane reactor with intermediate water removal could be an appropriate option for the ODHE process.

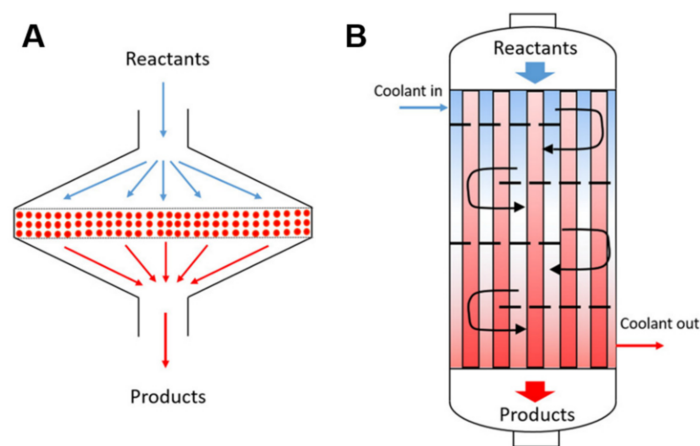


**Figure 23.** Schematics of (A) shallow pancake-like packed bed autothermal reactor and (B) long cooled multi-tubular reactor with a low depth-to-diameter ratio for the oxidative dehydrogenation of ethane. Adapted from ref. [134], Copyright (2020), with permission from John Wiley & Sons.

Baroi et al. [136] systematically evaluated the impact of feedstock composition on the operating cost, profitability, and process safety of ODHE based on M1 catalysts (as shown in Figure 24). The whole process was evaluated under different operating conditions, where no kinetic considerations were involved, catalytic performance was obtained from references, and the reactor was assumed as a black box. Based on the simulations, they proposed a staged oxygen feed process to minimize nitrogen and vapor in the gas stream, and the use of membrane separators made the process more profitable and safer. Moreover, they suggested that the use of  $\text{CO}_2$  as an oxidant is expected to be enhanced.

### 3.2.3. Selective Oxidation of Ethane over M1 Catalyst via a CL-ODH Process

Considering the separation and safety features, the conversion of ethane to ethylene by a chemical looping process has attracted the attention of researchers in the last few years [137–140], which also can be combined with a fluidized bed reactor [141], as shown in Figure 25. Mishanin et al. [142] used an  $\text{MoVNbTeO}_x$  catalyst to convert ethane to ethylene in a cyclic mode, which can also be considered as a chemical cyclic conversion process. The feed is alternated between ethane and air, and the ethane is converted by the lattice oxygen species of the M1 phase. The lattice oxygen species available for ethane conversion is increased with the temperature. Luongo et al. [143] developed a cyclic chemical-looping-based ODHE process by combining a  $\text{NaNO}_3$ -modified perovskite  $\text{Sr}_{0.8}\text{Ca}_{0.2}\text{FeO}_{3-\delta}$  as the oxygen carrier with the highly selective M1 catalysts to convert ethane. The  $\text{Sr}_{0.8}\text{Ca}_{0.2}\text{FeO}_{3-\delta}$  has a low ethylene selectivity in the process of ethane

feed only; however, it can release oxygen in the reduction process. Therefore, they used  $\text{Sr}_{0.8}\text{Ca}_{0.2}\text{FeO}_{3-\delta}$  as an oxygen carrier and utilized  $\text{NaNO}_3$  to suppress the  $\text{CO}_x$  formation during the CL-ODH process. The modified oxygen carrier (which can release oxygen during CL-ODH) is then combined with an excellent M1 catalyst to achieve highly selective ethane conversion under uncoupled oxygen conditions. Compared with the conventional ODHE over M1 phase and CL-ODH process with only perovskite  $\text{Sr}_{0.8}\text{Ca}_{0.2}\text{FeO}_{3-\delta}$  oxygen carrier, the combination of highly selective M1 phase with high oxygen carrier ability perovskite  $\text{Sr}_{0.8}\text{Ca}_{0.2}\text{FeO}_{3-\delta}$  allows this process being operated under the oxygen uncoupled condition and transfer the problem of ethylene selectivity for oxygen storage materials under CL-ODHE conditions into the inhibition of  $\text{CO}_x$  generation. Therefore, it brings new insights into the development of CL-ODH catalysts, i.e., catalysts for ethane oxidative dehydrogenation reactions and oxygen carriers can be optimized independently, thus reducing the difficulty of catalyst development.

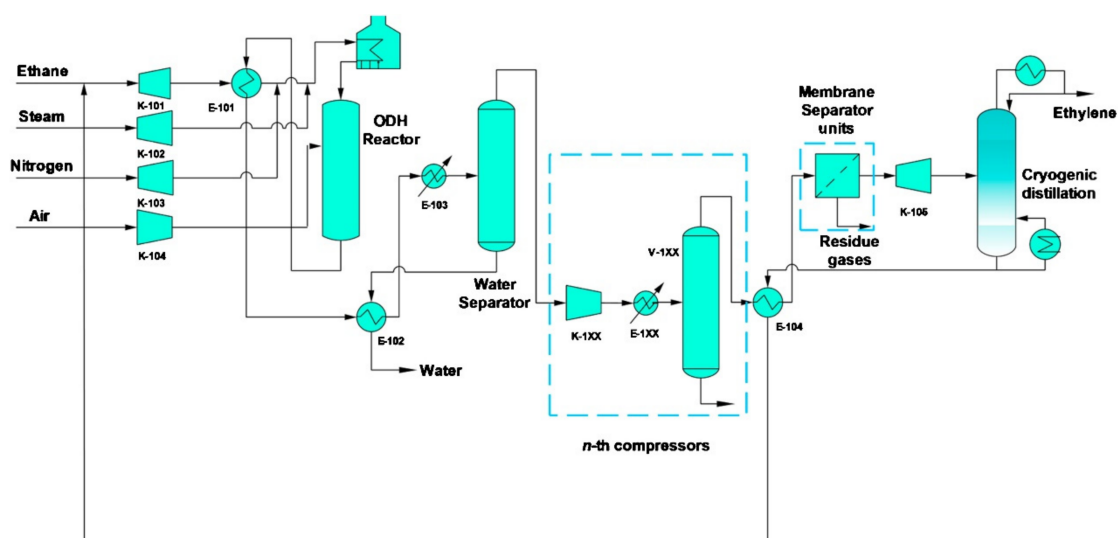


Figure 24. Overall generalized process flow diagram of the ODH process. Adapted from ref. [137], Copyright (2017), with permission from Elsevier.

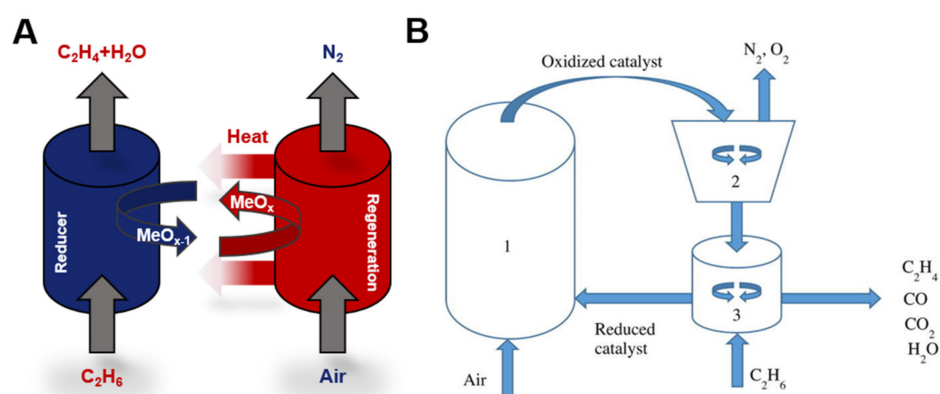


Figure 25. (A) Schematic for CL-ODH of ethane, and (B) ODHE in a fluidized bed reactor, Adapted from ref. [141], Copyright (2015), with permission from Elsevier.

#### 4. Concluding Remarks and Outlook

Along with the growing concern about global warming, the inevitable  $\text{CO}_2$  emissions from fossil fuels have caused great uncertainty in the development of the petrochemical industry. ODHE is a promising process for producing ethylene from abundant shale/natural gas resources, which is competitive with conventional steam cracking processes. However,

the industrialization of the ODHE process is still limited by the catalysts. In the past decade, the ODHE process over Mo-V-Nb-Te-based multi-component oxide has attracted tremendous research interest worldwide. The M1 catalyst-based ODHE process seems to be more attractive in small-scale plants to utilize dispersed ethane resources (e.g., associated LPG, which is usually treated by combustion).

For the M1 MoVNbTeO<sub>x</sub> catalysts itself, the ethane is activated on the basal surface of the M1 phase (or the one-dimensional heptagonal pores exposed on that surface), following the MvK redox mechanism. Although much work has been done to demonstrate the importance of vanadium abundance (V<sup>5+</sup>, the active sites for activation of light alkanes), it is believed that the catalytic performance per unit mass of catalyst is more relevant to the amounts of active sites and rate of the redox (turn-over frequency, TOF) [136]. Therefore, the enhancement of active sites, active surface per unit mass of catalysts, and improved redox properties will contribute to the catalytic performance, which can promote the development of the ODHE process over M1 MoVNbTeO<sub>x</sub> catalysts. Due to the complexity of Mo-V-Nb-Te multi-component oxide catalysts, the development of such catalysts is a time-consuming and laborious task. Despite the tremendous developments in DFT theoretical calculations, it is still not possible to achieve bottom-up catalyst design by means of theoretical calculations, and extensive laboratory validation work is still needed. A high throughput automatic screening process of catalysts combined with hardware and algorithms may be able to accelerate the development of catalysts. In the future, in situ characterization and theoretical calculations are important for the understanding at the molecular level, which can facilitate the development of catalysts on a laboratory scale. The optimization of catalyst synthesis procedures, reactor types, and the ODHE process based on M1 catalysts are important for the development of ethane oxidative dehydrogenation towards industrial implementation.

For reasons of operational safety in plants, the oxidation of ethane by soft oxidants seems to be more attractive. The growing concern about global warming has led to an investment in research on CO<sub>2</sub> conversion, and lots of work has been devoted to the selective oxidation of ethane by CO<sub>2</sub> [136,144–146]. However, due to the physical-chemical properties of M1 catalysts, there is still no published work on the ODHE by soft oxidant, which may be limited by the unsuitable operation temperature of the M1 phase catalysts and the activation of CO<sub>2</sub> molecule and can be achieved in a plasma-assisted catalytic process. For the concern of oxygen separation load and operational safety in plants, the chemical-looping process seems to be promising in the future.

**Author Contributions:** Writing—original draft preparation Y.C. (Yuxin Chen); writing—review and editing, Y.C. (Yuxin Chen), B.Y. and Y.C. (Yi Cheng); visualization, Y.C. (Yuxin Chen); supervision, Y.C. (Yi Cheng); funding acquisition, Y.C. (Yi Cheng). All authors have read and agreed to the published version of the manuscript.

**Funding:** This work is financially supported by the National Natural Science Foundation of China (No. 21776156 and No. 21991104).

**Data Availability Statement:** There is no new data created.

**Acknowledgments:** Yi Cheng would like to thank Jaap C. Schouten, Tjeerd Alexander Nijhuis and Lara Truter for their collaboration in the early stage of this research work, as well as his students, Bozhao Chu, Xin Chen, Dan Dang, and Shuairan Qian for their contributions to this ODHE project.

**Conflicts of Interest:** The authors declare that they have no known competing financial interest or personal relationship that could have appeared to influence the work reported in this paper.

## References

1. Gaffney, A.M.; Mason, O.M. Ethylene production via oxidative dehydrogenation of ethane using M1 catalyst. *Catal. Today* **2017**, *285*, 159–165. [[CrossRef](#)]
2. Jiang, M.; Zhang, M.; Wang, L.; Fei, Y.; Wang, S.; Núñez-Delgado, A.; Bokhari, A.; Race, M.; Khataee, A.; Jaromír Klemeš, J.; et al. Photocatalytic degradation of xanthate in flotation plant tailings by TiO<sub>2</sub>/graphene nanocomposites. *Chem. Eng. J.* **2022**, *431*, 134104. [[CrossRef](#)]

3. Han, N.; Wang, S.; Yao, Z.; Zhang, W.; Zhang, X.; Zeng, L.; Chen, R. Superior three-dimensional perovskite catalyst for catalytic oxidation. *EcoMat* **2020**, *2*, e12044. [[CrossRef](#)]
4. Han, N.; Feng, S.; Guo, W.; Mora, O.M.; Zhao, X.; Zhang, W.; Xie, S.; Zhou, Z.; Liu, Z.; Liu, Q.; et al. Rational design of ruddlesden–popper perovskite electrocatalyst for oxygen reduction to hydrogen peroxide. *SusMat* **2022**, *2*, 456–465. [[CrossRef](#)]
5. Feng, K.; Tian, J.; Zhang, J.; Li, Z.; Chen, Y.; Luo, K.H.; Yang, B.; Yan, B. Dual functionalized interstitial N atoms in  $\text{Co}_3\text{Mo}_3\text{N}$  enabling  $\text{CO}_2$  activation. *ACS Catal.* **2022**, *12*, 4696–4706. [[CrossRef](#)]
6. Bhasin, M.M. Is true ethane oxydehydrogenation feasible? *Top. Catal.* **2003**, *23*, 145–149. [[CrossRef](#)]
7. Sanfilippo, D.; Miracca, I. Dehydrogenation of paraffins: Synergies between catalyst design and reactor engineering. *Catal. Today* **2006**, *111*, 133–139. [[CrossRef](#)]
8. Cavani, F.; Ballarini, N.; Cericola, A. Oxidative dehydrogenation of ethane and propane: How far from commercial implementation? *Catal. Today* **2007**, *127*, 113–131. [[CrossRef](#)]
9. Gartner, C.A.; van Veen, A.C.; Lercher, J.A. Oxidative dehydrogenation of ethane: Common principles and mechanistic aspects. *ChemCatChem* **2013**, *5*, 3196–3217. [[CrossRef](#)]
10. Baca, M.; Pigamo, A.; Dubois, J.L.; Millet, J.M.M. Propane oxidation on MoVTeNbO mixed oxide catalysts: Study of the phase composition of active and selective catalysts. *Top. Catal.* **2003**, *23*, 39–46. [[CrossRef](#)]
11. López Nieto, J.M.; Botella, P.; Solsona, B.; Oliver, J.M. The selective oxidation of propane on Mo-V-Te-Nb-O catalysts: The influence of Te-precursor. *Catal. Today* **2003**, *81*, 87–94. [[CrossRef](#)]
12. Li, X.; Buttrey, D.J.; Blom, D.A.; Vogt, T. Improvement of the structural model for the M1 phase Mo–V–Nb–Te–O propane (amm)oxidation catalyst. *Top. Catal.* **2011**, *54*, 614–626. [[CrossRef](#)]
13. Kolen'ko, Y.V.; Zhang, W.; d'Alnoncourt, R.N.; Girgsdies, F.; Hansen, T.W.; Wolfram, T.; Schlögl, R.; Trunschke, A. Synthesis of MoVTeNb oxide catalysts with tunable particle dimensions. *ChemCatChem* **2011**, *3*, 1597–1606. [[CrossRef](#)]
14. Hävecker, M.; Wrabetz, S.; Kröhnert, J.; Csepei, L.-I.; Naumann d'Alnoncourt, R.; Kolen'ko, Y.V.; Girgsdies, F.; Schlögl, R.; Trunschke, A. Surface chemistry of phase-pure M1 MoVTeNb oxide during operation in selective oxidation of propane to acrylic acid. *J. Catal.* **2012**, *285*, 48–60. [[CrossRef](#)]
15. Celaya Sanfiz, A.; Hansen, T.W.; Sakthivel, A.; Trunschke, A.; Schlögl, R.; Knoester, A.; Brongersma, H.H.; Looi, M.H.; Hamid, S.B.A. How important is the (001) plane of M1 for selective oxidation of propane to acrylic acid? *J. Catal.* **2008**, *258*, 35–43. [[CrossRef](#)]
16. Melzer, D.; Xu, P.; Hartmann, D.; Zhu, Y.; Browning, N.D.; Sanchez-Sanchez, M.; Lercher, J.A. Atomic-scale determination of active facets on the MoVTeNb oxide M1 phase and their intrinsic catalytic activity for ethane oxidative dehydrogenation. *Angew. Chem. Int. Ed. Engl.* **2016**, *55*, 8873–8877. [[CrossRef](#)]
17. Chu, B.; An, H.; Chen, X.; Cheng, Y. Phase-pure M1 MoVNbTeO<sub>x</sub> catalysts with tunable particle size for oxidative dehydrogenation of ethane. *Appl. Catal. A Gen.* **2016**, *524*, 56–65. [[CrossRef](#)]
18. Chen, Y.; Qian, S.; Feng, K.; Li, Z.; Yan, B.; Cheng, Y. Determination of highly active and selective surface for the oxidative dehydrogenation of ethane over phase-pure M1 MoVNbTeO<sub>x</sub> catalyst. *J. Catal.* **2022**, *416*, 277–288. [[CrossRef](#)]
19. Chen, X.; Yang, Q.; Chu, B.; An, H.; Cheng, Y. Valence variation of phase-pure M1 MoVNbTe oxide by plasma treatment for improved catalytic performance in oxidative dehydrogenation of ethane. *RSC Adv.* **2015**, *5*, 91295–91301. [[CrossRef](#)]
20. Chu, B.; An, H.; Nijhuis, T.A.; Schouten, J.C.; Cheng, Y. A self-redox pure-phase M1 MoVNbTeO/CeO<sub>2</sub> nanocomposite as a highly active catalyst for oxidative dehydrogenation of ethane. *J. Catal.* **2015**, *329*, 471–478. [[CrossRef](#)]
21. Chu, B.; Truter, L.; Nijhuis, T.A.; Cheng, Y. Performance of phase-pure M1 MoVNbTeO catalysts by hydrothermal synthesis with different post-treatments for the oxidative dehydrogenation of ethane. *Appl. Catal. A Gen.* **2015**, *498*, 99–106. [[CrossRef](#)]
22. Chu, B.; Truter, L.; Nijhuis, T.A.; Cheng, Y. Oxidative dehydrogenation of ethane to ethylene over phase-pure M1 MoVNbTeO<sub>x</sub> catalysts in a micro-channel reactor. *Catal. Sci. Technol.* **2015**, *5*, 2807–2813. [[CrossRef](#)]
23. Dang, D.; Chen, X.; Yan, B.; Li, Y.; Cheng, Y. Catalytic performance of phase-pure M1 MoVNbTeO<sub>x</sub>/CeO<sub>2</sub> composite for oxidative dehydrogenation of ethane. *J. Catal.* **2018**, *365*, 238–248. [[CrossRef](#)]
24. Chen, X.; Dang, D.; An, H.; Chu, B.; Cheng, Y. MnOx promoted phase-pure M1 MoVNbTe oxide for ethane oxidative dehydrogenation. *J. Taiwan Inst. Chem. Eng.* **2019**, *95*, 103–111. [[CrossRef](#)]
25. Chen, Y.; Dang, D.; Yan, B.; Cheng, Y. Mixed metal oxides of M1 MoVNbTeO<sub>x</sub> and TiO<sub>2</sub> as composite catalyst for oxidative dehydrogenation of ethane. *Catalysts* **2022**, *12*, 71. [[CrossRef](#)]
26. Chen, Y.; Dang, D.; Yan, B.; Cheng, Y. Nanocomposite catalysts of non-purified MoVNbTeO<sub>x</sub> with CeO<sub>2</sub> or TiO<sub>2</sub> for oxidative dehydrogenation of ethane. *Chem. Eng. Sci.* **2022**, *264*, 118154. [[CrossRef](#)]
27. Chen, Y.; Qian, S.; Feng, K.; Wang, Y.; Yan, B.; Cheng, Y. MoVNbTeO<sub>x</sub> M1@CeO<sub>2</sub>@Cordierite structured catalysts for ODHE process. *Chem. Eng. Sci.* **2022**, *253*, 117597. [[CrossRef](#)]
28. Dang, D.; Chen, Y.; Chen, X.; Feng, K.; Yan, B.; Cheng, Y. Phase-pure M1 MoVNbTeO<sub>x</sub>/TiO<sub>2</sub> nanocomposite catalysts: High catalytic performance for oxidative dehydrogenation of ethane. *Catal. Sci. Technol.* **2022**, *12*, 1211–1219. [[CrossRef](#)]
29. Qian, S.; Chen, Y.; Wang, Y.; Yan, B.; Cheng, Y. Identification of the intrinsic active site in phase-pure M1 catalysts for oxidation dehydrogenation of ethane by density functional theory calculations. *J. Phys. Chem. C* **2022**, *126*, 17536–17543. [[CrossRef](#)]
30. Qian, S.; Chen, Y.; Yan, B.; Cheng, Y. Plasma treated M1 MoVNbTeO–CeO<sub>2</sub> composite catalyst for improved performance of oxidative dehydrogenation of ethane. *Green Energy Environ.* **2022**. [[CrossRef](#)]

31. Yan, P.; Chen, Y.; Cheng, Y. Industrially potential MoVNbTeO<sub>x</sub>@FoamSiC structured catalyst for oxidative dehydrogenation of ethane. *Chem. Eng. J.* **2022**, *427*, 131813. [[CrossRef](#)]
32. Thorsteinson, E.M.; Wilson, T.P.; Young, F.G.; Kasai, P.H. The oxidative dehydrogenation of ethane over catalysts containing mixed oxides of molybdenum and vanadium. *J. Catal.* **1978**, *52*, 116–132. [[CrossRef](#)]
33. McCain, J.H.; Charleston, W.V. Process for Oxygendhydrogenation of Ethane to Ethylene. U.S. Patent No. 4524236, 18 June 1985.
34. Ushikubo, T.; Nakamura, H.; Koyasu, Y.; Wajiki, S. Method for Producing an Unstaurated Carboxylic acid. U.S. Patent No. 5380933, 10 January 1995.
35. Ushikubo, T.; Oshima, K.; Ihara, T.; Amatsu, H. Method for Producing a Nitrile. U.S. Patent No. 5534650, 9 July 1996.
36. Ushikubo, T.; Oshima, K.; Kayou, A.; Vaarkamp, M.; Hatano, M. Ammoxidation of propane over catalysts comprising mixed oxides of Mo and V. *J. Catal.* **1997**, *169*, 394–396. [[CrossRef](#)]
37. Chen, N.F.; Oshihara, K.; Ueda, W. Selective oxidation of ethane over hydrothermally synthesized Mo–V–Al–Ti oxide catalyst. *Catal. Today* **2001**, *64*, 121–128. [[CrossRef](#)]
38. Ueda, W.; Oshihara, K. Selective oxidation of light alkanes over hydrothermally synthesized Mo–V–M–O (M = Al, Ga, Bi, Sb, and Te) oxide catalysts. *Appl. Catal. A Gen.* **2000**, *200*, 135–143. [[CrossRef](#)]
39. Oshihara, K.; Hisano, T.; Ueda, W. Catalytic oxidative activation of light alkanes over Mo–V-based oxides having controlled surface. *Top. Catal.* **2001**, *15*, 153–160. [[CrossRef](#)]
40. Watanabe, H.; Koyasu, Y. New synthesis route for Mo–V–Nb–Te mixed oxides catalyst for propane ammoxidation. *Appl. Catal. A Gen.* **2000**, *194*, 479–485. [[CrossRef](#)]
41. Xie, Q.; Chen, L.; Weng, W.; Wan, H. Preparation of MoVTe(Sb)Nb mixed oxide catalysts using a slurry method for selective oxidative dehydrogenation of ethane. *J. Mol. Catal. A Chem.* **2005**, *240*, 191–196. [[CrossRef](#)]
42. Grasselli, R.K.; Buttrey, D.J.; DeSanto, P.; Burrington, J.D.; Lugmair, C.G.; Volpe, A.F.; Weingand, T. Active centers in Mo–V–Nb–Te–O (amm)oxidation catalysts. *Catal. Today* **2004**, *91–92*, 251–258. [[CrossRef](#)]
43. DeSanto, P.; Buttrey, D.J.; Grasselli, R.K.; Lugmair, C.G.; Volpe, A.F.; Toby, B.H.; Vogt, T. Structural aspects of the M1 and M2 phases in MoVNbTeO propane ammoxidation catalysts. *Z. Kristall.* **2004**, *219*, 152–165. [[CrossRef](#)]
44. DeSanto Jr, P.; Buttrey, D.J.; Grasselli, R.K.; Lugmair, C.G.; Volpe, A.F.; Toby, B.H.; Vogt, T. Structural characterization of the orthorhombic phase M1 in MoVNbTeO propane ammoxidation catalyst. *Top. Catal.* **2003**, *23*, 23–38. [[CrossRef](#)]
45. Valente, J.S.; Armendáriz-Herrera, H.; Quintana-Solórzano, R.; del Ángel, P.; Nava, N.; Massó, A.; López Nieto, J.M. Chemical, structural, and morphological changes of a MoVTeNb catalyst during oxidative dehydrogenation of ethane. *ACS Catal.* **2014**, *4*, 1292–1301. [[CrossRef](#)]
46. Aouine, M.; Dubois, J.L.; Millet, J.M.M. Crystal chemistry and phase composition of the MoVTeNbO catalysts for the ammoxidation of propane. *Chem. Commun.* **2001**, 1180–1181. [[CrossRef](#)]
47. Millet, J.M.M.; Baca, M.; Pigamo, A.; Vitry, D.; Ueda, W.; Dubois, J.L. Study of the valence state and coordination of antimony in MoVSbO catalysts determined by XANES and EXAFS. *Appl. Catal. A Gen.* **2003**, *244*, 359–370. [[CrossRef](#)]
48. Shiju, N.R.; Liang, X.; Weimer, A.W.; Liang, C.; Dai, S.; Gulians, V.V. The role of surface basal planes of layered mixed metal oxides in selective transformation of lower alkanes: Propane ammoxidation over surface ab planes of Mo–V–Te–Nb–O M1 phase. *J. Am. Chem. Soc.* **2008**, *130*, 5850–5851. [[CrossRef](#)]
49. Konya, T.; Katou, T.; Murayama, T.; Ishikawa, S.; Sadakane, M.; Buttrey, D.; Ueda, W. An orthorhombic Mo<sub>3</sub>VO<sub>x</sub> catalyst most active for oxidative dehydrogenation of ethane among related complex metal oxides. *Catal. Sci. Technol.* **2013**, *3*, 380–387. [[CrossRef](#)]
50. Baca, M.; Aouine, M.; Dubois, J.; Millet, J. Synergetic effect between phases in MoVTe(Sb)NbO catalysts used for the oxidation of propane into acrylic acid. *J. Catal.* **2005**, *233*, 234–241. [[CrossRef](#)]
51. Holmberg, J.; Grasselli, R.K.; Andersson, A. A study of the functionalities of the phases in Mo–V–Nb–Te oxides for propane ammoxidation. *Top. Catal.* **2003**, *23*, 55–63. [[CrossRef](#)]
52. He, Q.; Woo, J.; Belianinov, A.; Gulians, V.V.; Borisevich, A.Y. Better catalysts through microscopy: Mesoscale M1/M2 intergrowth in molybdenum–vanadium based complex oxide catalysts for propane ammoxidation. *ACS Nano* **2015**, *9*, 3470–3478. [[CrossRef](#)]
53. Korovchenko, P.; Shiju, N.R.; Dozier, A.K.; Graham, U.M.; Guerrero-Pérez, M.O.; Gulians, V.V. M1 to M2 phase transformation and phase cooperation in bulk mixed metal Mo–V–M–O (M = Te, Nb) catalysts for selective ammoxidation of propane. *Top. Catal.* **2008**, *50*, 43–51. [[CrossRef](#)]
54. Deniau, B.; Bergeret, G.; Jouguet, B.; Dubois, J.L.; Millet, J.M.M. Preparation of single M1 phase MoVTe(Sb)NbO catalyst: Study of the effect of M2 phase dissolution on the structure and catalytic properties. *Top. Catal.* **2008**, *50*, 33–42. [[CrossRef](#)]
55. Baca, M.; Millet, J.M.M. Bulk oxidation state of the different cationic elements in the MoVTe(Sb)NbO catalysts for oxidation or ammoxidation of propane. *Appl. Catal. A Gen.* **2005**, *279*, 67–77. [[CrossRef](#)]
56. Híbst, H.; Rosowski, F.; Cox, G. New Cs-containing Mo–V<sup>4+</sup> based oxides with the structure of the M1 phase—Base for new catalysts for the direct alkane activation. *Catal. Today* **2006**, *117*, 234–241. [[CrossRef](#)]
57. Liu, Y.; McGill, C.J.; Green, W.H.; Deshlahra, P. Effects of surface species and homogeneous reactions on rates and selectivity in ethane oxidation on oxide catalysts. *AIChE J.* **2021**, *67*, e17483. [[CrossRef](#)]
58. Kardash, T.Y.; Lazareva, E.; Svintsitskiy, D.A.; Ishchenko, A.V.; Bondareva, V.M.; Neder, R.B. The evolution of the M1 local structure during preparation of VMoNbTeO catalysts for ethane oxidative dehydrogenation to ethylene. *RSC Adv.* **2018**, *8*, 35903–35916. [[CrossRef](#)] [[PubMed](#)]

59. Celaya Sanfiz, A.; Hansen, T.W.; Girgsdies, F.; Timpe, O.; Rödel, E.; Ressler, T.; Trunschke, A.; Schlögl, R. Preparation of phase-pure M1 MoVTeNb oxide catalysts by hydrothermal synthesis—Influence of reaction parameters on structure and morphology. *Top. Catal.* **2008**, *50*, 19–32. [[CrossRef](#)]
60. Grasselli, R.K.; Buttrey, D.J.; Burrington, J.D.; Andersson, A.; Holmberg, J.; Ueda, W.; Kubo, J.; Lugmair, C.G.; Volpe, A.F. Active centers, catalytic behavior, symbiosis and redox properties of MoV(Nb, Ta)TeO ammoxidation catalysts. *Top. Catal.* **2006**, *38*, 7–16. [[CrossRef](#)]
61. Mars, P.; van Krevelen, D.W. Oxidations carried out by means of vanadium oxide catalysts. *Chem. Eng. Sci.* **1954**, *3*, 41–59. [[CrossRef](#)]
62. Aouine, M.; Epicier, T.; Millet, J.-M.M. In situ environmental STEM study of the MoVTe oxide M1 phase catalysts for ethane oxidative dehydrogenation. *ACS Catal.* **2016**, *6*, 4775–4781. [[CrossRef](#)]
63. Watanabe, N.; Ueda, W. Comparative study on the catalytic performance of single-phase Mo–V–O-based metal oxide catalysts in propane ammoxidation to acrylonitrile. *Ind. Eng. Chem. Res.* **2006**, *45*, 607–614. [[CrossRef](#)]
64. Rahman, F.; Loughlin, K.F.; Al-Saleh, M.A.; Saeed, M.R.; Tukur, N.M.; Hossain, M.M.; Karim, K.; Mamedov, A. Kinetics and mechanism of partial oxidation of ethane to ethylene and acetic acid over MoV type catalysts. *Appl. Catal. A Gen.* **2010**, *375*, 17–25. [[CrossRef](#)]
65. Deniau, B.; Nguyen, T.T.; Delichere, P.; Safonova, O.; Millet, J.M.M. Redox state dynamics at the surface of MoVTe(Sb)NbO M1 phase in selective oxidation of light alkanes. *Top. Catal.* **2013**, *56*, 1952–1962. [[CrossRef](#)]
66. Girgsdies, F.; Schlögl, R.; Trunschke, A. In-situ X-ray diffraction study of phase crystallization from an amorphous MoVTeNb oxide catalyst precursor. *Catal. Commun.* **2012**, *18*, 60–62. [[CrossRef](#)]
67. Xin, C.; Wang, F.; Xu, G.Q. Tuning surface V<sup>5+</sup> concentration in M1 phase MoVSbO<sub>x</sub> catalysts for ethylene production from ethane through oxidative dehydrogenation reaction. *Appl. Catal. A Gen.* **2021**, *610*, 117946. [[CrossRef](#)]
68. López Nieto, J.M.; Botella, P.; Concepción, P.; Dejoz, A.; Vázquez, M.I. Oxidative dehydrogenation of ethane on Te-containing MoVNbO catalysts. *Catal. Today* **2004**, *91–92*, 241–245. [[CrossRef](#)]
69. Botella, P.; García-González, E.; López Nieto, J.M.; González-Calbet, J.M. MoVTeNbO multifunctional catalysts: Correlation between constituent crystalline phases and catalytic performance. *Solid State Sci.* **2005**, *7*, 507–519. [[CrossRef](#)]
70. Nguyen, T.T.; Aouine, M.; Millet, J.M.M. Optimizing the efficiency of MoVTeNbO catalysts for ethane oxidative dehydrogenation to ethylene. *Catal. Commun.* **2012**, *21*, 22–26. [[CrossRef](#)]
71. Botella, P.; Dejoz, A.; Abello, M.C.; Vázquez, M.I.; Arrúa, L.; López Nieto, J.M. Selective oxidation of ethane: Developing an orthorhombic phase in Mo–V–X (X = Nb, Sb, Te) mixed oxides. *Catal. Today* **2009**, *142*, 272–277. [[CrossRef](#)]
72. Sanfiz, A.C.; Hansen, T.W.; Teschner, D.; Schnörch, P.; Girgsdies, F.; Trunschke, A.; Schlögl, R.; Looi, M.H.; Hamid, S.B.A. Dynamics of the MoVTeNb oxide M1 phase in propane oxidation. *J. Phys. Chem. C* **2010**, *114*, 1912–1921. [[CrossRef](#)]
73. Naraschewski, F.N.; Praveen Kumar, C.; Jentys, A.; Lercher, J.A. Phase formation and selective oxidation of propane over MoVTeNbO<sub>x</sub> catalysts with varying compositions. *Appl. Catal. A Gen.* **2011**, *391*, 63–69. [[CrossRef](#)]
74. Blom, D.A.; Li, X.; Mitra, S.; Vogt, T.; Buttrey, D.J. STEM HAADF image simulation of the orthorhombic M1 phase in the Mo–V–Nb–Te–O propane oxidation catalyst. *ChemCatChem* **2011**, *3*, 1028–1033. [[CrossRef](#)]
75. Murayama, H.; Vitry, D.; Ueda, W.; Fuchs, G.; Anne, M.; Dubois, J.L. Structure characterization of orthorhombic phase in MoVTeNbO catalyst by powder X-ray diffraction and XANES. *Appl. Catal. A Gen.* **2007**, *318*, 137–142. [[CrossRef](#)]
76. Pyrz, W.D.; Blom, D.A.; Shiju, N.R.; Gulians, V.V.; Vogt, T.; Buttrey, D.J. Using aberration-corrected STEM imaging to explore chemical and structural variations in the M1 phase of the MoVNbTeO oxidation catalyst. *J. Phys. Chem. C* **2008**, *112*, 10043–10049. [[CrossRef](#)]
77. Pyrz, W.D.; Blom, D.A.; Vogt, T.; Buttrey, D.J. Direct imaging of the MoVTeNbO M1 phase using an aberration-corrected high-resolution scanning transmission electron microscope. *Angew. Chem. Int. Ed. Engl.* **2008**, *47*, 2788–2791. [[CrossRef](#)] [[PubMed](#)]
78. Concepción, P.; Hernández, S.; López Nieto, J.M. On the nature of active sites in MoVTeO and MoVTeNbO catalysts: The influence of catalyst activation temperature. *Appl. Catal. A Gen.* **2011**, *391*, 92–101. [[CrossRef](#)]
79. Fu, G.; Xu, X.; Lu, X.; Wan, H. Mechanisms of initial propane activation on molybdenum oxides: A density functional theory study. *J. Phys. Chem. B* **2005**, *109*, 6416–6421. [[CrossRef](#)]
80. Gulians, V.V.; Bhandari, R.; Brongersma, H.H.; Knoester, A.; Gaffney, A.M.; Han, S. A study of the surface region of the Mo–V–Te–O catalysts for propane oxidation to acrylic acid. *J. Phys. Chem. B* **2005**, *109*, 10234–10242. [[CrossRef](#)] [[PubMed](#)]
81. Zhang, W.; Trunschke, A.; Schlögl, R.; Su, D. Real-space observation of surface termination of a complex metal oxide catalyst. *Angew. Chem. Int. Ed. Engl.* **2010**, *49*, 6084–6089. [[CrossRef](#)]
82. Trunschke, A.; Noack, J.; Trojanov, S.; Girgsdies, F.; Lunkenbein, T.; Pfeifer, V.; Hävecker, M.; Kube, P.; Sprung, C.; Rosowski, F.; et al. The impact of the bulk structure on surface dynamics of complex Mo–V-based oxide catalysts. *ACS Catal.* **2017**, *7*, 3061–3071. [[CrossRef](#)]
83. Zhu, Y.; Sushko, P.V.; Melzer, D.; Jensen, E.; Kovarik, L.; Ophus, C.; Sanchez-Sanchez, M.; Lercher, J.A.; Browning, N.D. Formation of oxygen radical sites on MoVNbTeO<sub>x</sub> by cooperative electron redistribution. *J. Am. Chem. Soc.* **2017**, *139*, 12342–12345. [[CrossRef](#)]
84. Melzer, D.; Mestl, G.; Wanninger, K.; Zhu, Y.; Browning, N.D.; Sanchez-Sanchez, M.; Lercher, J.A. Design and synthesis of highly active MoVTeNb-oxides for ethane oxidative dehydrogenation. *Nat. Commun.* **2019**, *10*, 4012. [[CrossRef](#)] [[PubMed](#)]
85. Panov, G.I.; Dubkov, K.A.; Starokon, E.V. Active oxygen in selective oxidation catalysis. *Catal. Today* **2006**, *117*, 148–155. [[CrossRef](#)]

86. Sadovskaya, E.; Goncharov, V.; Popova, G.; Ishchenko, E.; Frolov, D.; Fedorova, A.; Andrushkevich, T. Mo-V-Te-Nb oxide catalysts: Reactivity of different oxygen species in partial and deep oxidation. *J. Mol. Catal. A Chem.* **2014**, *392*, 61–66. [[CrossRef](#)]
87. Sadakane, M.; Ohmura, S.; Kodato, K.; Fujisawa, T.; Kato, K.; Shimidzu, K.-I.; Murayama, T.; Ueda, W. Redox tunable reversible molecular sieves: Orthorhombic molybdenum vanadium oxide. *Chem. Commun.* **2011**, *47*, 10812–10814. [[CrossRef](#)] [[PubMed](#)]
88. Ishikawa, S.; Yi, X.; Murayama, T.; Ueda, W. Catalysis field in orthorhombic Mo<sub>3</sub>VO<sub>x</sub> oxide catalyst for the selective oxidation of ethane, propane and acrolein. *Catal. Today* **2014**, *238*, 35–40. [[CrossRef](#)]
89. Ishikawa, S.; Yi, X.D.; Murayama, T.; Ueda, W. Heptagonal channel micropore of orthorhombic Mo<sub>3</sub>VO<sub>x</sub> as catalysis field for the selective oxidation of ethane. *Appl. Catal. A Gen.* **2014**, *474*, 10–17. [[CrossRef](#)]
90. Ishikawa, S.; Kobayashi, D.; Konya, T.; Ohmura, S.; Murayama, T.; Yasuda, N.; Sadakane, M.; Ueda, W. Redox treatment of orthorhombic Mo<sub>29</sub>V<sub>11</sub>O<sub>112</sub> and relationships between crystal structure, microporosity and catalytic performance for selective oxidation of ethane. *J. Phys. Chem. C* **2015**, *119*, 7195–7206. [[CrossRef](#)]
91. Annamalai, L.; Ezenwa, S.; Dang, Y.; Tan, H.; Suib, S.L.; Deshlahra, P. Comparison of structural and catalytic properties of monometallic Mo and V oxides and M1 phase mixed oxides for oxidative dehydrogenation. *Catal. Today* **2021**, *368*, 28–45. [[CrossRef](#)]
92. Annamalai, L.; Liu, Y.; Ezenwa, S.; Dang, Y.; Suib, S.L.; Deshlahra, P. Influence of tight confinement on selective oxidative dehydrogenation of ethane on MoVTeNb mixed oxides. *ACS Catal.* **2018**, *8*, 7051–7067. [[CrossRef](#)]
93. Liu, Y.; Annamalai, L.; Deshlahra, P. Effects of lattice O atom coordination and pore confinement on selectivity limitations for ethane oxidative dehydrogenation catalyzed by vanadium-oxo species. *J. Phys. Chem. C* **2019**, *123*, 28168–28191. [[CrossRef](#)]
94. Liu, Y.; Twombly, A.; Dang, Y.; Mirich, A.; Suib, S.L.; Deshlahra, P. Roles of enhancement of C–H activation and diminution of C–O formation within M1-phase pores in propane selective oxidation. *ChemCatChem* **2020**, *13*, 882–899. [[CrossRef](#)]
95. López-Medina, R.; Sobczak, I.; Golinska-Mazwa, H.; Ziolk, M.; Bañares, M.A.; Guerrero-Pérez, M.O. Spectroscopic surface characterization of MoVNbTe nanostructured catalysts for the partial oxidation of propane. *Catal. Today* **2012**, *187*, 195–200. [[CrossRef](#)]
96. Heine, C.; Hävecker, M.; Sanchez-Sanchez, M.; Trunschke, A.; Schlögl, R.; Eichelbaum, M. Work function, band bending, and microwave conductivity studies on the selective alkane oxidation catalyst MoVTeNb oxide (orthorhombic M1 phase) under operation conditions. *J. Phys. Chem. C* **2013**, *117*, 26988–26997. [[CrossRef](#)]
97. Naumann d’Alnoncourt, R.; Csepei, L.-I.; Hävecker, M.; Girgsdies, F.; Schuster, M.E.; Schlögl, R.; Trunschke, A. The reaction network in propane oxidation over phase-pure MoVTeNb M1 oxide catalysts. *J. Catal.* **2014**, *311*, 369–385. [[CrossRef](#)]
98. Kubas, A.; Noak, J.; Trunschke, A.; Schlogl, R.; Neese, F.; Maganas, D. A combined experimental and theoretical spectroscopic protocol for determination of the structure of heterogeneous catalysts: Developing the information content of the resonance Raman spectra of M1 MoVOx. *Chem. Sci.* **2017**, *8*, 6338–6353. [[CrossRef](#)] [[PubMed](#)]
99. Svintsitskiy, D.A.; Kardash, T.Y.; Lazareva, E.V.; Saraev, A.A.; Derevyannikova, E.A.; Vorokhta, M.; Šmíd, B.; Bondareva, V.M. NAP-XPS and in situ XRD study of the stability of Bi-modified MoVNbTeO catalysts for oxidative dehydrogenation of ethane. *Appl. Catal. A Gen.* **2019**, *579*, 141–150. [[CrossRef](#)]
100. Ramírez-Salgado, J.; Quintana-Solórzano, R.; Mejía-Centeno, I.; Armendáriz-Herrera, H.; Rodríguez-Hernández, A.; Guzmán-Castillo, M.d.L.; Valente, J.S. On the role of oxidation states in the electronic structure via the formation of oxygen vacancies of a doped MoVTeNbOx in propylene oxidation. *Appl. Surf. Sci.* **2022**, *573*, 151428. [[CrossRef](#)]
101. Al-Ghamdi, S.; Volpe, M.; Hossain, M.M.; de Lasa, H. VO<sub>x</sub>/c-Al<sub>2</sub>O<sub>3</sub> catalyst for oxidative dehydrogenation of ethane to ethylene: Desorption kinetics and catalytic activity. *Appl. Catal. A Gen.* **2013**, *450*, 120–130. [[CrossRef](#)]
102. Cheng, M.J.; Goddard, W.A., 3rd. In silico design of highly selective Mo-V-Te-Nb-O mixed metal oxide catalysts for ammoxidation and oxidative dehydrogenation of propane and ethane. *J. Am. Chem. Soc.* **2015**, *137*, 13224–13227. [[CrossRef](#)]
103. Cheng, M.J.; Goddard, W.A. The mechanism of alkane selective oxidation by the M1 phase of Mo–V–Nb–Te mixed metal oxides: Suggestions for improved catalysts. *Top. Catal.* **2016**, *59*, 1506–1517. [[CrossRef](#)]
104. Grabowski, R. Kinetics of oxidative dehydrogenation of C<sub>2</sub>–C<sub>3</sub> alkanes on oxide catalysts. *Catal. Rev.* **2006**, *48*, 199–268. [[CrossRef](#)]
105. Valente, J.S.; Quintana-Solórzano, R.; Armendáriz-Herrera, H.; Barragán-Rodríguez, G.; López-Nieto, J.M. Kinetic study of oxidative dehydrogenation of ethane over MoVTeNb mixed-oxide catalyst. *Ind. Eng. Chem. Res.* **2013**, *53*, 1775–1786. [[CrossRef](#)]
106. Che-Galicia, G.; Quintana-Solorzano, R.; Ruiz-Martinez, R.S.; Valente, J.S.; Castillo-Araiza, C.O. Kinetic modeling of the oxidative dehydrogenation of ethane to ethylene over a MoVTeNbO catalytic system. *Chem. Eng. J.* **2014**, *252*, 75–88. [[CrossRef](#)]
107. Donaubaue, P.J.; Melzer, D.M.; Wanninger, K.; Mestl, G.; Sanchez-Sanchez, M.; Lercher, J.A.; Hinrichsen, O. Intrinsic kinetic model for oxidative dehydrogenation of ethane over MoVTeNb mixed metal oxides: A mechanistic approach. *Chem. Eng. J.* **2020**, *383*, 123195. [[CrossRef](#)]
108. Gaffney, A.M.; Sims, J.W.; Martin, V.J.; Duprez, N.V.; Louthan, K.J.; Roberts, K.L. Evaluation and analysis of ethylene production using oxidative dehydrogenation. *Catal. Today* **2021**, *369*, 203–209. [[CrossRef](#)]
109. Kubo, J.; Watanabe, N.; Ueda, W. Propane ammoxidation with lattice oxygen of Mo–V–O-based complex metal oxide catalysts. *Chem. Eng. Sci.* **2008**, *63*, 1648–1653. [[CrossRef](#)]
110. De Arriba, A.; Solsona, B.; Dejoz, A.M.; Concepción, P.; Homs, N.; de la Piscina, P.R.; López Nieto, J.M. Evolution of the optimal catalytic systems for the oxidative dehydrogenation of ethane: The role of adsorption in the catalytic performance. *J. Catal.* **2022**, *408*, 388–400. [[CrossRef](#)]

111. Grant, J.T.; Venegas, J.M.; McDermott, W.P.; Hermans, I. Aerobic oxidations of light alkanes over solid metal oxide catalysts. *Catal. Rev.* **2018**, *118*, 2769–2815. [CrossRef]
112. Mestl, G.; Margittfalvi, J.L.; Végvári, L.; Szijjártó, G.P.; Tompos, A. Combinatorial design and preparation of transition metal doped MoVTe catalysts for oxidation of propane to acrylic acid. *Appl. Catal. A Gen.* **2014**, *474*, 3–9. [CrossRef]
113. Hernández-Morejudo, S.; Massó, A.; García-González, E.; Concepción, P.; López Nieto, J.M. Preparation, characterization and catalytic behavior for propane partial oxidation of Ga-promoted MoVTeO catalysts. *Appl. Catal. A Gen.* **2015**, *504*, 51–61. [CrossRef]
114. Ishchenko, E.V.; Kardash, T.Y.; Gulyaev, R.V.; Ishchenko, A.V.; Sobolev, V.I.; Bondareva, V.M. Effect of K and Bi doping on the M1 phase in MoVTeNbO catalysts for ethane oxidative conversion to ethylene. *Appl. Catal. A Gen.* **2016**, *514*, 1–13. [CrossRef]
115. Yun, Y.S.; Lee, M.; Sung, J.; Yun, D.; Kim, T.Y.; Park, H.; Lee, K.R.; Song, C.K.; Kim, Y.; Lee, J.; et al. Promoting effect of cerium on MoVTeNb mixed oxide catalyst for oxidative dehydrogenation of ethane to ethylene. *Appl. Catal. B Environ.* **2018**, *237*, 554–562. [CrossRef]
116. Ishchenko, E.V.; Gulyaev, R.V.; Kardash, T.Y.; Ishchenko, A.V.; Gerasimov, E.Y.; Sobolev, V.I.; Bondareva, V.M. Effect of Bi on catalytic performance and stability of MoVTeNbO catalysts in oxidative dehydrogenation of ethane. *Appl. Catal. A Gen.* **2017**, *534*, 58–69. [CrossRef]
117. Lazareva, E.V.; Bondareva, V.M.; Svintsitskiy, D.A.; Ishchenko, A.V.; Marchuk, A.S.; Kovalev, E.P.; Kardash, T.Y. Oxidative dehydrogenation of ethane over M1 MoVNbTeO catalysts modified by the addition of Nd, Mn, Ga or Ge. *Catal. Today* **2021**, *361*, 50–56. [CrossRef]
118. Zhou, Y.; Lin, J.; Li, L.; Tian, M.; Li, X.; Pan, X.; Chen, Y.; Wang, X. Improving the selectivity of Ni-Al mixed oxides with isolated oxygen species for oxidative dehydrogenation of ethane with nitrous oxide. *J. Catal.* **2019**, *377*, 438–448. [CrossRef]
119. Najari, S.; Saeidi, S.; Concepcion, P.; Dionysiou, D.D.; Bhargava, S.K.; Lee, A.F.; Wilson, K. Oxidative dehydrogenation of ethane: Catalytic and mechanistic aspects and future trends. *Chem. Soc. Rev.* **2021**, *50*, 4564–4605. [CrossRef] [PubMed]
120. Zenkovets, G.A.; Shutilov, A.A.; Bondareva, V.M.; Sobolev, V.I.; Marchuk, A.S.; Tsybulya, S.V.; Prosvirin, I.P.; Ishchenko, A.V.; Gavrilov, V.Y. New multicomponent MoVSbNbCeO<sub>x</sub>/SiO<sub>2</sub> catalyst with enhanced catalytic activity for oxidative dehydrogenation of ethane to ethylene. *ChemCatChem* **2020**, *12*, 4149–4159. [CrossRef]
121. López-Medina, R.; Guerrero-Pérez, M.O.; Bañares, M.A. Nanosized-bulk V-containing mixed-oxide catalysts: A strategy for the improvement of the catalytic materials properties. *New J. Chem.* **2019**, *43*, 17661–17669. [CrossRef]
122. Massó Ramírez, A.; Ivars-Barceló, F.; López Nieto, J.M. Optimizing reflux synthesis method of Mo-V-Te-Nb mixed oxide catalysts for light alkane selective oxidation. *Catal. Today* **2020**, *356*, 322–329. [CrossRef]
123. Ramli, I.; Botella, P.; Ivars, F.; Pei Meng, W.; Zawawi, S.M.M.; Ahangar, H.A.; Hernández, S.; Nieto, J.M.L. Reflux method as a novel route for the synthesis of MoVTeNbOx catalysts for selective oxidation of propane to acrylic acid. *J. Mol. Catal. A Chem.* **2011**, *342–343*, 50–57. [CrossRef]
124. Fan, Y.; Li, S.; Liu, Y.; Wang, Y.; Wang, Y.; Chen, Y.; Yu, S. High-pressure hydrothermal synthesis of MoVTeNbOx with high surface V<sup>5+</sup> abundance for oxidative conversion of propane to acrylic acid. *J. Supercrit. Fluids* **2022**, *181*, 105469. [CrossRef]
125. Wang, Y.; Fan, Y.; Li, S.; Wang, Y.; Chen, Y.; Liu, D.; Wei, W.; Yu, S. Crystal structure and catalytic performance for direct oxidation of propylene to acrylic acid of MoVTeNbOx prepared by high-pressure hydrothermal synthesis. *Resour. Chem. Mater.* **2022**, *1*, 211–221. [CrossRef]
126. Li, S.; Liu, Y.; Fan, Y.; Lu, Z.; Yan, Y.; Deng, L.; Zhang, Z.; Yu, S. Facile sub-/supercritical water synthesis of nanoflake MoVTeNbO x-mixed metal oxides without post-heat treatment and their catalytic performance. *RSC Adv.* **2020**, *10*, 39922–39930. [CrossRef] [PubMed]
127. Yi, J.P.; Fan, Z.G.; Jiang, Z.W.; Li, W.S.; Zhou, X.P. High-throughput parallel reactor system for propylene oxidation catalyst investigation. *J. Comb. Chem.* **2007**, *9*, 1053–1059. [CrossRef] [PubMed]
128. Bergh, S.; Cong, P.; Ehnebuske, B.; Guan, S.; Hagemeyer, A.; Lin, H.; Liu, Y.; Lugmair, C.G.; Turner, H.W.; Volpe, A.F., Jr.; et al. Combinatorial heterogeneous catalysis: Oxidative dehydrogenation of ethane to ethylene, selective oxidation of ethane to acetic acid, and selective ammoxidation of propane to acrylonitrile. *Top. Catal.* **2003**, *23*, 65–79. [CrossRef]
129. Zhu, H.; Laveille, P.; Rosenfeld, D.C.; Hedhili, M.N.; Basset, J.-M. A high-throughput reactor system for optimization of Mo-V-Nb mixed oxide catalyst composition in ethane ODH. *Catal. Sci. Technol.* **2015**, *5*, 4164–4173. [CrossRef]
130. Dalian Institute of Chemical Technology—Wison Engineering’s Joint Development of Ethane Oxidative Dehydrogenation to Ethylene Technology Passed Pilot Technical Evaluation. Available online: <http://www.wison-engineering.com/site/newsDetail/305> (accessed on 13 September 2021).
131. Nguyen, T.T.; Burel, L.; Nguyen, D.L.; Pham-Huu, C.; Millet, J.M.M. Catalytic performance of MoVTeNbO catalyst supported on SiC foam in oxidative dehydrogenation of ethane and ammoxidation of propane. *Appl. Catal. A Gen.* **2012**, *433*, 41–48. [CrossRef]
132. Lin, J.; Tian, J.; Cheng, X.; Tan, J.; Wan, S.; Lin, J.; Wang, Y. Propane ammoxidation over MoVTeNb oxide catalyst in a microchannel reactor. *AIChE J.* **2018**, *64*, 4002–4008. [CrossRef]
133. Che-Galicia, G.; Ruiz-Martínez, R.S.; López-Isunza, F.; Castillo-Araiza, C.O. Modeling of oxidative dehydrogenation of ethane to ethylene on a MoVTeNbO/TiO<sub>2</sub> catalyst in an industrial-scale packed bed catalytic reactor. *Chem. Eng. J.* **2015**, *280*, 682–694. [CrossRef]
134. Chen, J.K.; Bollini, P.; Balakotaiah, V. Oxidative dehydrogenation of ethane over mixed metal oxide catalysts: Autothermal or cooled tubular reactor design? *AIChE J.* **2021**, *67*, e17168. [CrossRef]

135. Fazlinezhad, A.; Naeimi, A.; Yasari, E. Theoretical investigation of ethane oxidative dehydrogenation over MoVTaNbO catalyst in fixed-bed reactors with intermediate water removal. *Chem. Eng. Res. Des.* **2019**, *146*, 427–435. [[CrossRef](#)]
136. Baroi, C.; Gaffney, A.M.; Fushimi, R. Process economics and safety considerations for the oxidative dehydrogenation of ethane using the M1 catalyst. *Catal. Today* **2017**, *298*, 138–144. [[CrossRef](#)]
137. Yusuf, S.; Neal, L.M.; Li, F. Effect of promoters on manganese-containing mixed metal oxides for oxidative dehydrogenation of ethane via a cyclic redox scheme. *ACS Catal.* **2017**, *7*, 5163–5173. [[CrossRef](#)]
138. Neal, L.M.; Haribal, V.P.; Li, F. Intensified ethylene production via chemical looping through an exergetically efficient redox scheme. *iScience* **2019**, *19*, 894–904. [[CrossRef](#)] [[PubMed](#)]
139. Chan, M.S.C.; Baldovi, H.G.; Dennis, J.S. Enhancing the capacity of oxygen carriers for selective oxidations through phase cooperation: Bismuth oxide and ceria–zirconia. *Catal. Sci. Technol.* **2018**, *8*, 887–897. [[CrossRef](#)]
140. Wu, T.; Yu, Q.; Roghair, I.; Wang, K.; van Sint Annaland, M. Chemical looping oxidative dehydrogenation of propane: A comparative study of Ga-based, Mo-based, V-based oxygen carriers. *Chem. Eng. Process. Process Intensif.* **2020**, *157*, 108137. [[CrossRef](#)]
141. Bakare, I.A.; Mohamed, S.A.; Al-Ghamdi, S.; Razzak, S.A.; Hossain, M.M.; de Lasa, H.I. Fluidized bed ODH of ethane to ethylene over VO<sub>x</sub>–MoO<sub>x</sub>/γ-Al<sub>2</sub>O<sub>3</sub> catalyst: Desorption kinetics and catalytic activity. *Chem. Eng. J.* **2015**, *278*, 207–216. [[CrossRef](#)]
142. Mishanin, I.I.; Kalenchuk, A.N.; Maslakov, K.I.; Lunin, V.V.; Koklin, A.E.; Finashina, E.D.; Bogdan, V.I. Oxidative dehydrogenation of ethane over a Mo–V–Nb–Te–O mixed-oxide catalyst in a cyclic mode. *Kinet. Catal.* **2017**, *58*, 156–160. [[CrossRef](#)]
143. Luongo, G.; Donat, F.; Bork, A.H.; Willinger, E.; Landuyt, A.; Müller, C.R. Highly selective oxidative dehydrogenation of ethane to ethylene via chemical looping with oxygen uncoupling through structural engineering of the oxygen carrier. *Adv. Energy Mater.* **2022**, *12*, 2200405. [[CrossRef](#)]
144. Liu, J.; He, N.; Zhang, Z.; Yang, J.; Jiang, X.; Zhang, Z.; Su, J.; Shu, M.; Si, R.; Xiong, G.; et al. Highly-dispersed zinc species on zeolites for the continuous and selective dehydrogenation of ethane with CO<sub>2</sub> as a soft oxidant. *ACS Catal.* **2021**, *11*, 2819–2830. [[CrossRef](#)]
145. Zhang, P.; Tong, J.; Huang, K. Role of CO<sub>2</sub> in catalytic ethane-to-ethylene conversion using a high-temperature CO<sub>2</sub> transport membrane reactor. *ACS Sustain. Chem. Eng.* **2019**, *7*, 6889–6897. [[CrossRef](#)]
146. Al-Mamoori, A.; Lawson, S.; Rownaghi, A.A.; Rezaei, F. Oxidative dehydrogenation of ethane to ethylene in an integrated CO<sub>2</sub> capture-utilization process. *Appl. Catal. B Environ.* **2020**, *278*, 119329. [[CrossRef](#)]

**Disclaimer/Publisher’s Note:** The statements, opinions and data contained in all publications are solely those of the individual author(s) and contributor(s) and not of MDPI and/or the editor(s). MDPI and/or the editor(s) disclaim responsibility for any injury to people or property resulting from any ideas, methods, instructions or products referred to in the content.